Towards Personal Fabricators: Tabletop tools for micron and sub-micron scale functional rapid prototyping.

Saul Griffith
B.Met.E. University of NSW, 1997.
ME, University of Sydney, 2000.

Submitted to the Program in Media Arts and Sciences School of Architecture and Planning in partial fulfillment of the requirements for the degree of
Master of Science in Media Arts and Sciences
at the Massachusetts Institute of Technology
February 2001

Written by **Saul Griffith**
Program in Media Arts and Sciences
September 30, 2000

Certified by **Joseph Jacobson**
Associate Professor
Program in Media Arts and Sciences
Department of Mechanical Engineering
Thesis Advisor

Accepted by **Stephen Benton**
Chair of Departmental Committee
on Graduate Students
Program in Media Arts and Sciences

Towards Personal Fabricators: Tabletop tools for micron and sub-micron scale functional rapid prototyping.

Saul Griffith

Submitted to the Program in Media Arts and Sciences,
School of Architecture and Planning,
On September 30, 2000,
in partial fulfillment of the requirements for the degree of
Master of Science in Media Arts and Sciences
Massachusetts Institute of Technology

Abstract

Three tools for the rapid prototyping of micron and sub-micron scale devices are presented. These tools represent methods for the manufacture of PEMS, or Printed micro Electro Mechanical Systems, and are enabled because they exploit the novel properties of nanocrystalline materials and their interactions with energetic beams. UV contact mask lithography was used to directly pattern metallic nanocrystals on glass and polyimide surfaces without vacuum or etching processes or the use of photoresist layers. Direct electron beam lithography of nanocrystalline metals was used to pattern multiple layer, multiple material, structures with minimum feature sizes of 100nm. Finally a micro-mirror array based selective laser sintering apparatus was built for the rapid, maskless patterning of PEMS. This tool was used to directly pattern metal structures, and for the rapid manufacture of elastomeric stamps for "nano embossing". Minimum feature sizes under 10 microns were achieved and routes to 2 micron features described. Processing time was reduced to hours from the weeks for traditional photomask / photolithography based systems. These tools are examined in the greater context of rapid prototyping technologies.

Thesis Advisor:

Joseph Jacobson
Associate Professor
Program in Media Arts and Sciences
Department of Mechanical Engineering

Towards Personal Fabricators: Tabletop tools for micron and sub-micron scale functional rapid prototyping.

Saul Griffith

Thesis Committee

Joseph Jacobson
Associate Professor
Program in Media Arts and Sciences
Department of Mechanical Engineering
Thesis Advisor

Neil Gershenfeld
Associate Professor
Program in Media Arts and Sciences
MIT Media Laboratory
Thesis Reader

Hiroshi Ishii
Associate Professor
Program in Media Arts and Sciences
MIT Media Laboratory
Thesis Reader

Towards Personal Fabricators: Tabletop tools for micron and sub-micron scale functional rapid prototyping.

Table of Contents

Table of Figures.

1 - Introduction

Computers have permeated our daily life to an extraordinary degree. Whereas it is often considered (indeed fashionably and almost tediously so) how this influences the information that passes through our lives, I believe an equally or more interesting question is how this influences the materials and things that are tangible parts of our lives. Despite the protestations and desires of some, we still live in a world of atoms, not a world of bits. Our world of bits is, however, increasingly influencing our arrangement of atoms – the way we make the things that we live with. Printers are now available in an extraordinary variety that can produce anything from postcards to billboards, three dimensional architectural models to boat sails. Indeed, at a different scale, the modern factory with its level of computerized automation could be considered - to a fashion - a printer.

Traditionally the word print is associated with the written word and with works on paper. The printing press is often accredited as one of the great inventions of mankind for its mass propagation and storage of knowledge by low cost production of duplicates. In an increasingly computerised world, the word printer has become associated with peripherals used for outputing information from the printer. Most typically this still means printed text and images on paper, but the emergence of tools such as stereo-lithography and laser-cutters has begun to challenge what can be a printer. As used in this piece, the word printer describes a machine that outputs a physical object entirely under computer control once it has been

designed by human – computer interaction and fed with raw materials. It is important that the property that multiple copies can be easily reproduced is retained, and in a world of increasing personalisation that the ability to produce many similar objects and iterations of an object is a feature. To reduce it to point form, a 'printer', should be a mechanism that:

- Modifies materials under computer control.
- Can produce multiple copies and minor variations of an object.
- Requires human interaction only in the loading of raw materials (eg. Loading a paper tray), and perhaps in part finishing (eg. Stapling a document).
- Produces a useful object, either aesthetically, structurally, *logically* or a combination thereof.

And perhaps the most important deviation from the traditional idea of a printer is that:

- The form, or pattern, can be rapidly changed. Printer now means to be able to change the output arbitrarily and in real time, not to wait on the production of new molds, type sets, or infrastructure.

The word printer is now indelibly associated with our desktop ink-jet or laser printer. Rapid prototyping is typically used to describe the general field of 3D printing or free form fabrication. Rapid prototyping within the title, and throughout this thesis refers to systems for rapidly printing or manufacturing an item that is usually a one of a kind or of a short run. Rapid fabrication is a more accurate term as the material advances in this field, and those in this thesis, suggest that these tools will be used to make final products not just test prototypes. Functional is used as a descriptor of the products of the printers built in this thesis. Specifically this is to differentiate this work which incorporates a broader array of materials including electronically functional materials into a 3D printing technology, as opposed to merely structural materials.

At a practical and an engineering level, this thesis is exploring a methodology, a suite of materials, and a group of technologies, for challenging what it is possible to print, specifically in the MEMS, or micron scale domain. Three prototype printing systems are introduced for the manufacture of non-silicon, many-layered, multiple material PEMS or Printed micro-Electro-Mechanical Systems. Presented is a system for the fabrication of sub-micron feature sized, multiple layer, and multiple material devices using electron beam lithography of nanocrystalline materials. A second system for the patterning of these same nanocrystalline materials via ultra-violet exposure through a contact mask. Finally, a maskless lithography system for the direct patterning of nanocrystalline materials and for the rapid production of elastomeric stamps for micro-contact printing is introduced.

Chapter 2 represents a brief history of 'printing' technologies and explores the many orders of magnitude over which humans manufacture things under automated control from computer based designs. Briefly introduced in this chapter is the author's work in other rapid prototyping and printing domains including an ultra-low cost three dimensional printer of chocolate and bee's wax, and a process for the rapid production (again based on a 'printing' technology) of individually tailored bicycles.

Chapter 3 introduces the technical specifics and prior art of MEMS manufacture focusing on techniques other than the photolithography of silicon which is by far the dominant paradigm. Chapter 4 goes on to introduce the chosen material systems used for the printing systems developed in this thesis. This chapter is an introduction to nanoparticulate colloids, their properties and processing characteristics.

Chapter 5 highlights early development work towards a PEMS technology including selective laser sintering, contact mask UV

lithography, and multi-layer electron beam lithography, of nanoparticle based materials. The work in this chapter is background to the maskless, micromirror array based, selective laser sintering and elastomeric stamp manufacturing system demonstrated in chapter 6.

2 - The Printing of things

Printing over orders of magnitude

Computer controlled manufacturing now spans such a diverse range of physical systems and objects that the most useful way to summarise them is by orders of magnitude. As one can see from the map below, printed objects now span over 10 orders of magnitude, at every scale at which man manufactures things. This is testimony to our desire for, and skill in, manipulating matter. For a more comprehensive treatment of the rapidly evolving field of rapid prototyping (of which 3D printing, automated fabrication, and solid freeform fabrication are subsets) the reader is referred to references 1 & 2.

The most elegant introduction to printing over orders of magnitude is Feynman's now legendary talk "There's plenty of room at the bottom"[3]. In this field defining invited talk to the American Physical Society at Caltech, Feynman outlined a methodology for building machines that build similar, smaller, machines, that build similar, smaller, machines, and so on, until the finest, atomic scale machines are produced. Technology has essentially done this with increasing effort at each scale in the reduction, however, we are yet to build a single machine that is capable of producing a working copy of itself without human intervention, let alone one capable of decreasing its scale repeatedly. Four decades have passed since Feynman's talk, with little progress towards implementing this vision. The difficulty, novelty, and ramifications of this task (machine reproduction) cannot be underestimated – the inspiration for this work, evolution

and DNA based organisms, took a billion years to achieve the same goal.

It is important to define here two categories of printing: reproductive printing, and flexible printing. Reproductive printing systems such as stamping and traditional photolithography utilize master patterns or masks from which many multiple copies are made. These master patterns and masks are tedious and expensive to prepare, much in the same way as the traditional lithographer's stone, or engraver's plate. Flexible printing systems, such as the ink-jet, use techniques that are implicitly flexible in their output because they are data driven; there is no master mold or plate - the design is pixel or bit based. To correct an error, or to iterate on a design does not require the manufacture of a new master and can be implemented in real time. In general the trade off between flexible and reproductive printing systems is one of variability versus speed in volume production, and accuracy.

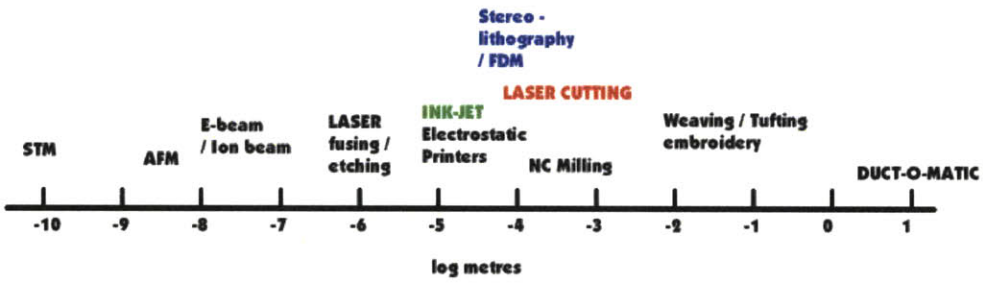

Figure 2.1. Orders of magnitude of printers.

Figure 2.1 provides a broad overview, scaled by order of magnitude in metres, of bit-based manufacturing. It is useful to look at each of these scales, and to push the analogy of the printer to see where it might prove useful. At one end of the scale we can see the manipulation of individual atoms in the STM work of Don Eigler, at the other, we see an industrial machine capable of taking raw sheetmetal and transforming it into complicated 3 dimensional ductwork structures. Combined with the tangible examples of

working processes listed below are conjectures as to future possibilities for the printing, or computer aided manufacture of a broadening array of tangible objects. Perhaps these will serve as stimuli for further research and discussion on the direction of such rapid prototyping technologies.

10^{-9}m – The STM

The honour of the finest scale 'printer' built to date should probably go to Eigler and Schweizer[4] for their famous manipulation of individual xenon atoms into the IBM logo with an STM tip. The STM tip was orginally invented by Binnig and Rohrer[5] for the imaging of surfaces with atomic resolution. Eigler and Schweizer trapped individual atoms at the STM tip by increasing tunnelling current at the tip when it was above a xenon atom. This effectively locked the atom to the tip while it was still loosely bound to the substrate. Under feedback control the atom could in this mode be pushed (or dragged) across the surface to desired positions. Eigler and Schweizer are the first to admit the limitations of this technique as a generic atomic building tool and obviously build times will be geologically slow (individual atoms are moved across the surface at 4 angstroms / second), however it is a promising move towards atomic control of matter.

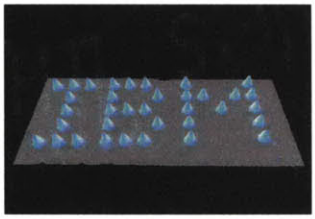

Figure 2.2 Xenon atoms arranged to form IBM logo. Eigler and Schweizer[4].

The limitations of the serial nature of all of the printing mechanisms described herein are most evident at this scale where the highly parallel replicative mechanisms of RNA-polymerase and DNA demonstrate amazing capacity for organizing large amounts of highly structured and multi-functional matter with a simple set of

building blocks. The most inspirational (and challenging to reproduce inorganically) aspect of the biological approach are built in mechanisms for error correction and the self assembly of large numbers of components. One meme of biological assembly worthy of note at this scale is the error prevention inherent in DNA replication. RNA-polymerase acts as a zipper in the linear denaturing of DNA. By reducing the replication of the structure to one linear dimension, errors are limited to 1 in 10^8. Subsequent to replication the mRNA codes for the assembly of 20 types of amino acids, again into a linear chain – this chain then folds into the three dimensional proteins that form the structural material, and enzymatic catalysts of life. Coding and replication is done in one dimension (error prevention) which then folds into three dimensions, allowing the highly parallel gathering of source materials (amino acids) in a three dimensional solution, to quickly assemble the larger more complicated structures that shape organisms.

10^{-8}m – The AFM

At a barely larger scale than the STM, the AFM is increasingly looking like a useful tool for lithographic and printing processes at the nanometer scale. In a similar fashion to the STM, X-rays, electron beams, and optics, the AFM was originally developed for imaging surfaces, before being used to manipulate them. The AFM was first developed by Binnig, Quate, and Gerber[6], combining the principles of the STM and a stylus profilometer. More recently it has become a cost effective mainstay of atomic scale imaging. Two methods of application highlight mechanisms for using it in a printing mode.

Field induced oxidation by STM probe tips was originally developed by Dagata et al.[7] and Sugimura[8] on silicon and titanium surfaces respectively. In this work, probe tips are bought into close proximity to a thin metal film then a bias voltage is applied to the tip to induce local oxidation in the presence of surface adsorbed water. The

resolution of this process is limited by the diameter of the probe tip and the surface roughness of the substrate. Cooper et.al.[9] increased the resolution of this process by employing a carbon nanotube attached to the probe tip and an atomically flat titanium surface on a (1A surface roughness) α-Al_2O_3 substrate. 8nm bits (TiO2) were written at 20nm pitch effectively giving a 1.6 Tbits/in^2 effective density if used in a memory application. This surface modification technique, although limited to oxides, can be used for the production of memory arrays and nanoscale devices such as single electron transistors.

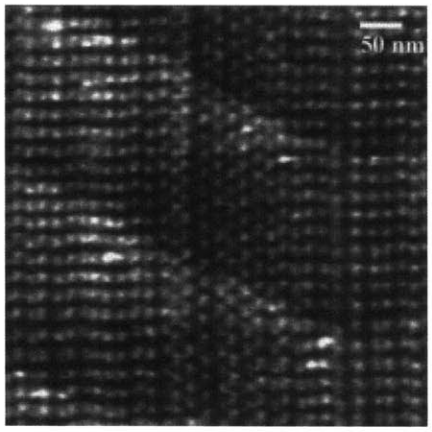

Figure 2.3. AFM image of terabit / sq. inch oxidised titanium surface. From Cooper99

Wilder et.al.[10,11] explored the use of AFM cantilevers and tips as electron sources for localised exposure of various photoresists. The resolution of electron beam lithography (EBL) is limited by back-scattering of the high-energy (10-100keV) electrons and the focusing optics. Proximity effects cause printed feature size to depend on local pattern density. The use of low energy electrons from a proximal probe can increase the resolution of scanning probe lithography (SPL) over EBL. A current feedback system is required in an AFM/STM lithography system to ensure constant electron dose as probe / surface distances and conditions change. Wilder et.al. used PMMA and a commercially available e-beam sensitized photoresist and achieved linewidths to 26nm. The resists were used as direct

etch masks and lift off masks for vapour deposited chrome. The SPL technique gives improved exposure latitude and narrower line widths than the EBL method. This is due to the fundamentally different process of electron interaction. In the EBL method, high energy electrons are decelerated through the resist whereas in the SPL, initially low energy electrons are accelerated through the resist by the field between tip and substrate. The field in the SPL technique is thought to confine scattering compared to EBL and hence the higher observed resolution in spite of the higher required dose of electrons.

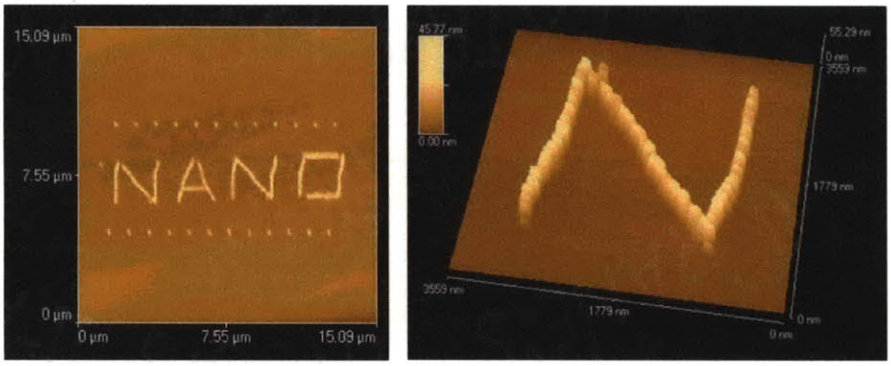

Figure 2.4. Depositional patterning of metals by AFM 'Nanostamping'. Hubert and Bletsas 2000.

Furthermore, recent unpublished work by Hubert and Bletsas[12], has indicated that the AFM can be used as a depositional tool, not just as a surface modification mechanism. In this manner they have increased the range of materials that can be deposited to most things in liquid or gel form with appropriate wetting characteristics. A further advantage of their technique is multilayer processing. In these techniques they are essentially using the probe tip as a stamp from which material is transferred to the substrate. The stamp can be repeatedly inked by being bought into contact with an appropriate source pool of material and redeposited in an additive printing step at another area. The build-time for this process is obviously slow, but routes to multiple tips and parrallel printing are conceivable, as are material feed mechanisms that supply the tip

directly rather than requiring repeated 're-inking' of the cantilever tip. This development can be likened to ink-jet printing, only at the nanometre rather than micrometre scale. Piner et.al.[13] used a similar method employing capillary forces to deposit alkanethiols on gold substrates with 30nm resolution.

10^{-7}m – Electron beams, Ion beams, deep UV lithography, microstamping.

Electron beam lithography (EBL) had its origins in photomask generation in the 60's (non98). EBL is still the primary method for generating photomasks for use in IC manufacture. EBL is fundamentally a serial process, as opposed to the parallel through mask processes of ion beam and optical lithography, and hence it is slow. Because it is not a mask based system however, it is a flexible printing system that can build arbitrary patterns in real time – though not practical for production of multiples. Direct writing of metallic nano, and micro, structures by electron beam is further discussed in chapter 5.

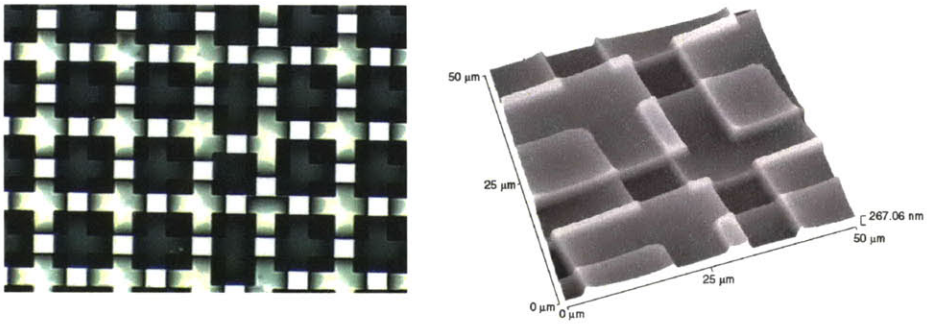

Figure 2.5. Optical micrograph and AFM image of nanoembossed, 2 layer structure. Courtesy C.Bulthaup.

Another route to printing that necessitates mention here is microstamping, or micro-contact printing. This process was pioneered by George Whitesides[14] at Harvard and is a flexible and low cost mechanism for patterning surfaces. It is a reproductive patterning technique suited to volume production as each mold must be manufactured from a silicon master. This process and its

derivatives are capable to resolutions below 50nm and reliably pattern over large areas at 200nm resolution. The three great challenges to these techniques are multilayer allignment, error free large areas, and truly 3 dimensional structures.

10^{-6}m – Optical lithography, MEMS and IC's

Optical lithography barely needs introduction, and as a technology is more than amply covered in many treatments of the subject [eg.15]. Optical lithography has its origins in photography. It has been pushed by, and heeded to, Moore's law, in an interesting case of technological supply and demand, where a stated trend became the desire and motivation for technical improvements that pushed the development of lasers, photo-polymers and optics, to levels that have consistently broken previous predictions of limits. In the current year, 2000, 1/4 micron lithography is routine, and experimental 197 and 153nm systems are bordering on industrial implementation.

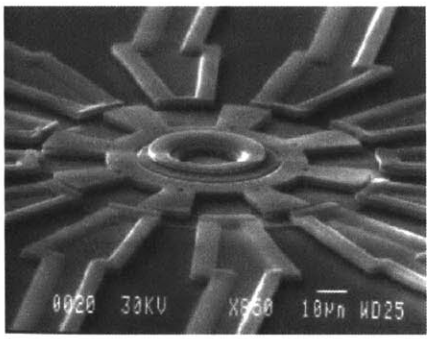

Figure 2.6. Traditional surface micromachined MEMS rotor by the MUMPS process. www.memsrus.com

Optical lithography is a versatile printing technique that has allowed the proliferation of personal computers and electronic devices and increasingly of MEMS devices. The processes involved are fundamentally limited to reproductive printing where expensive master mask sets are used to produce many multiple copies. In this sense it is not a printing process by the definition of this thesis, yet its use is so prolific in the domain that the printing systems developed herein are used that it necessitates mention.

The complexity of equipment and process in optical lithography routes to MEMS and IC's cannot be stressed enough in terms of creating rapid prototyping routes to devices in these domains. Traditional optical lithography processing of MEMS and IC's requires high purity, crystalline Si substrates, high temperature processing, vacuum deposition steps, chemical and plasma etching and stringent cleanliness requirements. All of these aspects lead to expensive and time consuming processing which is particularly limiting in terms of long turn around times on prototype developments.

10^{-5}m – Ink Jets, laser printers, and the desktop

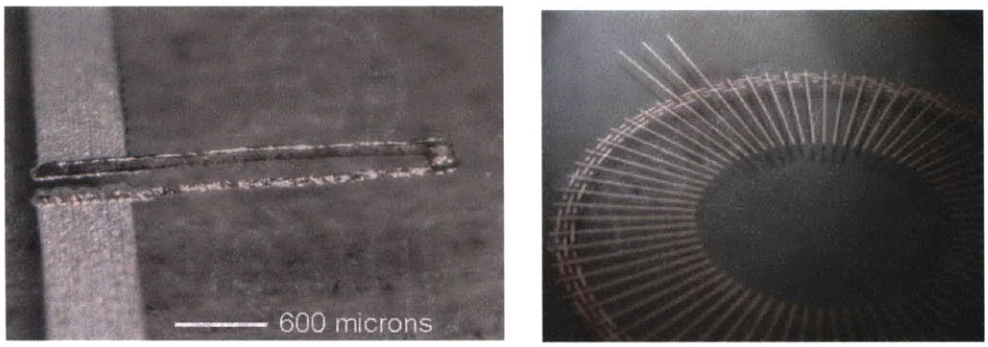

Figure 2.7. Ink jetted thermal 'heatuator' and rotary electrostatic motor including insulators. Courtesy Sawyer Fuller.

Sawyer Fuller[16], of the Micromedia group at MIT discusses in his thesis the use of ink-jet technologies for the additive fabrication of sub-millimetre scale electro-mechanical systems. This work can be seen to have its origins in the work of Paul Williams[17] whose work led to many developments in ink-jet based 3D prototyping including the company Z-corp. Fuller's work describes the novel use of colloidal suspensions of nanoparticulate materials where high metal loadings and properties described elsewhere in this thesis lead to high performance mechanical and electrical structures. A 20-100 micron limit on the resolution of ink-jet deposited structures is apparent, though many areas of application fit in this range, and the highly

parallel and well developed technology of ink-jetting bodes well for low cost and broad application.

10^{-4}m – Stereolithography and rapid prototyping

Burns, and Jacobs, in their respective books[1,2], introduce these domains at length. It is at this size domain of fraction of millimetre resolution, and hand and head sized objects that the most development work in terms of three dimensional printing has occurred including a number of commercially available machines from companies such as Stratasys and Z-corp. These machines typically find application in industrial prototyping.

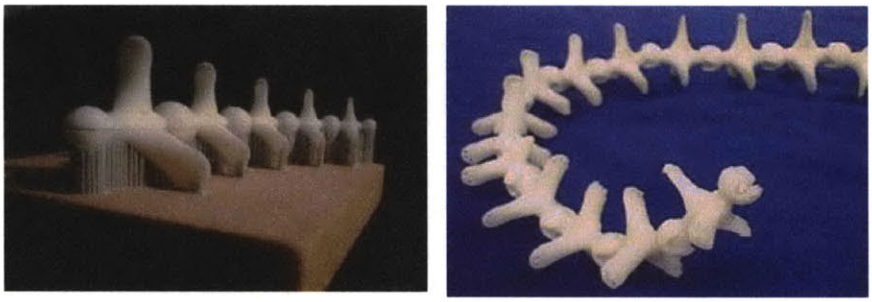

Figure 2.8. An articulated three dimensional spine by FDM. Author's design 1999. The upper image includes the foam substrate and printed supporting material that are later removed.

Three main technologies exist for building truly three dimensional objects. The first is stereolithography in photopolymerizable resin. By this technique a laser is scanned over the surface of a bath of resin inducing local curing. The cured material is on a stage that is lowered into the bath revealing a fresh uncured surface layer for the next layer in the process. The liquid bath acts as the support for the complex growing objects. Stratasys markets a system based on Fused Depositional Modeling (FDM) in which a bead of softened thermoplastic is extruded from a nozzle onto a substrate. The head is scanned in X and Y axes and at the completion of a layer the stage is lowered for subsequent layers. Two materials are used, the second is another thermoplastic or water-soluble material that is used to build pillared support structures for overhangs and cantilevers. The

second material is removed upon finishing to reveal the finished part. The third main process utilizes ink-jet printing to deposit resin in a powdered bed. Again, the resin is deposited in a two dimensional layer and fused whereupon a new layer of powdered material is deposited for the next layer in the stack. In this process the powdered bed acts as the supporting structure for subsequent layers. The powdered bed process has the greatest material versatility as powdered metals can be deposited and sintered to produce close to fully dense products. Each process has advantages and disadvantages based on materials available, build time, and surface finish. It is useful to note that in all processes defining three dimensional objects a 'release' layer or support material that is later removed is necessary for building any structure that has overhang (eg. A cantilever.) The images at left are of a fully articulated – as printed – spine from a FDM machine. This article serves as inspiration for printing moving, actuated objects.

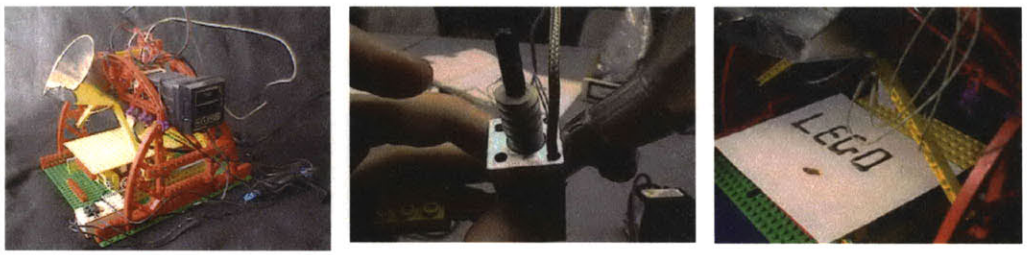

Figure 2.9. A sub $100 3D printer of chocolate or wax. Author's own work

One of the impediments to greater application of 3D printers (as this class of machines is generally called) is cost. Industrial models typically run at tens of thousands of dollars and up. With the aim of reducing this cost two orders of magnitude to tens or at most a hundred dollars the author undertook to build a working printer using that humblest of engineering toolkits – LEGO. With a simple extrusion chamber based on a worm screw, and three axis actuation based upon the LEGO robotics motors and the LOGO programming platform, a printer capable of printing in chocolate and beeswax (inherently cheap and recycleable materials) was built. The Printer can be seen at left. A simple thermocouple / PLD controlled bar

heater combination were used for temperature control of the extrusion chamber (detail at left). A three dimensional printer using programming languages designed for children and low cost consumables has been implemented. One can imagine a new paradigm for children's toys involving the child in the design, production, and then eating! of their own play-things.

10^{-3}m – NC machining – Milling and turning

The first application of computer aided manufacture, with a history of 50 years use, is NC (Numerically Controlled) machining. This technology is so pervasive it barely needs mention here except perhaps as the nucleus of this field. NC milling and turning has developed beyond mere prototyping into manufacture and encompasses all machineable materials. Of important note with all such processes is their subtractive nature which contrasts to the additive fabrication of stereolithography. Subtractive processes limit the geometry of articles to realizeable toolpaths that exclude hollow, socketed, and articulated parts. 5 and 6 axis machines are now common that attempt to overcome these limits, but at the expense of high cost and complexity.

10^{-1}m – Laser and Water jet cutting

At this 0.1 - 1m, very human sized scale, I believe some of the most fun and interesting possibilities for new printers lies. This is the size of our everyday objects, the size at which we physically interact with the world. The emergence of a laser cutter in the basement of the Media Laboratory has seen an extraordinary range of experimentation with hand and head sized objects and particularly in building personalized interfaces for a wide array of computer applications. Laser and water jet cutters, although limited to cutting planar sheets, allow for 3 dimensional object construction by appropriate use of lamination, grooves, and keys.

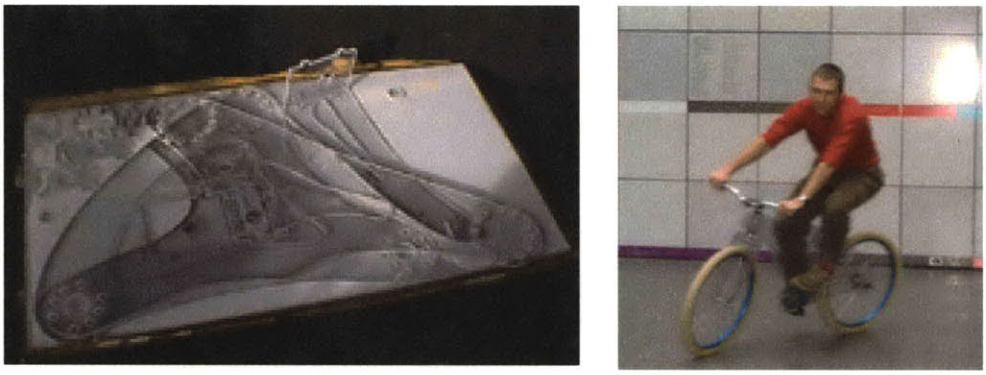

Figure 2.10. Water jet cut, polycarbonate bicycle. Layered sheets and assembled, ride-able bicycle. Author's work, 1999.

At this scale it is possible to 'print' moving things. From laser cutting patterns in the textiles used for making parafoil kites to water jet cutting bicycles. A water jet cut bicycle from polycarbonate sheet is shown at left. The keyed components were easily assembled by squeeze fit into a working fork and frame set. Traditional alloy cranks, bottom bracket, wheels, and chain were employed, although conceptually one can imagine ways to make almost all of these components by printing methods. The bicycle making exercise points to both the freedoms and limitations of printing manufacture. A lot of freedom was granted in the aesthetic and structural design, though at the same time the structural design had to account for the fundamentally low mechanical properties of extruded polycarbonate when compared to traditional bicycle frame materials. It can be said of all printing type processes and modes of flexible manufacture that they represent a compromise in structural integrity and materials processing. Work hardening, heat treatment, forging, and other processing based material property modifications are not inherent in the printing processes described though they may be moderately applied post printing.

Plasma, laser, and water jet cutting machines employed at this scale result in a much lower entry to manufacture and customisation. Without doubt smaller scale prototyping tools of similar accessibility would allow for a higher degree of creativity in MEMS scale devices.

10^0m – Large objects and specialized printers for industrial niches.

Salvagnini s.p.a of Italy fabricate a completely automated assembly line[1] printer, the S4+P4, for the punching, nibbling, and bending of sheet metal into three dimensional objects such as desks, drawers, refrigerator bodies, light housings and the like. A similar venture is that of Iowa Precision that manufactures the 'Fabriduct', a machine that takes raw metal sheet and fibreglass insulation input, and outputs completely folded and partially assembled heating, ventilation, and air conditioning, duct work. Both of these systems allow for in-line changing of the design files such that new component designs are output at the push of a button.

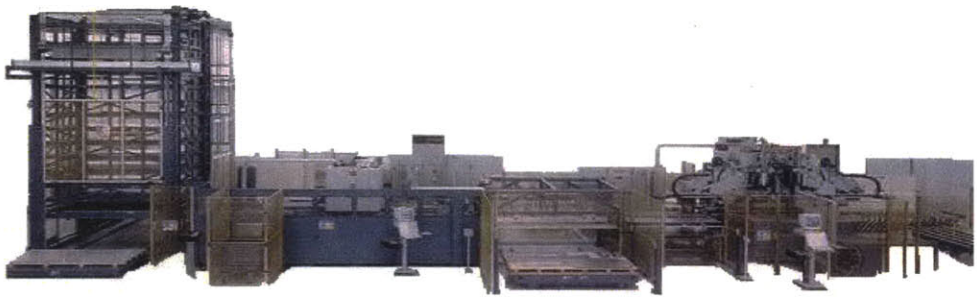

Figure 2.11. Salvagnini's S4P4 flexible sheet metal fabricator

Wilcom-Tecos, a company with origins in the CAM operation of embroidery machines, now offers CAM operation of carpet tufting machinery. These carpet tufters have a bed size up to 6x9 metres and have the capacity to individually place single tufted yarns of different colour and length over that area.

Disney imagineering engineers talk of the use of a CAM steel re-bar bending machine that takes files of artificial mountains, and reproduces the appropriate formwork structure for subsequent concrete rendering into extremely large physical structures (50m x 50m and up).

These examples point to the utility of automated fabrication or printing type modes of manufacture in the flexibility they offer in

terms of modified or personalized items within a range or domain of products. As the scale of production increases it is at the cost of material and product flexibility. The above systems are obviously specialised for certain products which points to the development of many such CAM mechanisms or 'printers' for large scale objects. Assembly steps are a requirement at this scale, however the discretisation of parts into individually handleable units can facilitate minimal heavy lifting or joining equipment in the assembly of entire structures. Without doubt we can expect a proliferation of domain specific computer controlled fabricators.

10^1m and beyond – The printing of truly big things: architectural structures.

At what scale does the printing analogy break down? The previous examples point to large two dimensional objects in the case of carpeting and limited three dimensional objects in the case of the Fabriduct sheetmetal working machine and programmed re-bar benders.

Figure 2.12. Model and first prototype of a printed paper school-house or emergency relief shelter. Pappu, Griffith, SCA, 2000.

Dow Chemical produced a self-generating styrofoam dome that essentially is a building printer[18,19]. A reaction vessel for the polymerisation and foaming of polystyrene is placed at the end of a beam that rotates around a central pole. By extruding a bead of foam as the beam rotates and moves up the pole a dome is created. These domes have been used to make medical clinics, and as emergency relief shelters after earthquakes in Nicaragua.

In collaboration with SCA and Ravi Pappu of MIT, the capacity to print a school, infrastructure and content included, that could be configured on site and rolled out of machinery that fitted on the back of a truck, was pursued. Paper is a surprisingly durable and versatile material and with modern corrugation and polymer coating techniques good mechanical and weathering or environmental properties can be obtained. Utilising printed text on all surfaces of the building, a large portion of a grade school curriculum can be included on the walls of the classroom, and on the desks and chairs of the furniture. For example, one wall can be printed with a world map and local geography, a second with a complete dictionary, and perhaps with multiple languages, a third with the principles of arithmetic, geometry, and calculus, the last with history and science. The ceiling could be printed as a planetarium or map of the universe and each chair and desk covered with a different novel or text book. The external walls of the structure could be printed with information that affects both the community and the class - healthcare, environmental care and monitoring, land management and sanitation. It is not difficult to imagine a single manufacturing truck that does the entire job with a laser cutter to cut the panels from cardboard sheet material and a large ink-jet printer to add the educational content. This allows each community to be involved in the architectural design and curriculum content in real-time.

A low cost three dimensional structure of cardboard such as this could also serve as a three dimensional blueprint for a more permanent structure. In the case of the schoolhouse, the cardboard framework could be laminated or veneered with local materials to become a more permanent structure, or with more research into the integrity of the material even become the formwork for pouring concrete or similar structural materials.

Further out again people have postulated the integral role of printer type manufacturing modes in the exploration of space. The impracticality of taking earth bound materials into space to use in building infrastructure for living temporarily or even settling is impractical and expensive. An efficient way of building a variety of objects from locally available feedstocks is one obvious route to take. Collection and processing of these materials will then obviously be important. With renewed interest in space exploration and particularly manned missions to Mars, these ideas will undoubtedly be revisited.

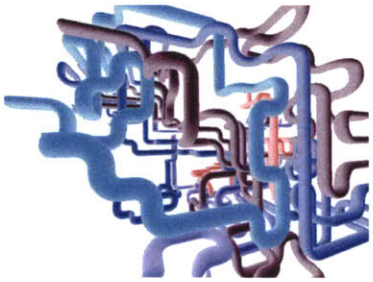

Figure 2.13. Printing outside of the box.

Perhaps the greatest challenge here is one of the ratio of printer scale to output product scale. In none of the examples I have mentioned and none of the processes I know is the volume of the printed object larger than the volume of the printer - excluding the schoolhouse or ductwork examples which require a large degree of human intervention to assemble the components into a larger structure. The printers mentioned so far work with enclosures or bounds larger than the printable object, to release the machine from such a paradigm a new approach is required, perhaps best illustrated by a screensaver!. The 3D pipes screensaver extrudes a tube of material in 3D space. This virtual manufacturing process has an analogue in the pultrusion process popular in the composite materials manufacturing industry. The pultrusion process employs a metal mold of a certain cross section through which fibres are pulled with a coating of thermo or photo curing resin that is kept in a bath

on the feed side of the mould. A small innovation from here is to drive the mould against the cured material it has just hardened and to draw new materials through the hollow core of the section. A physical version of the 3D pipes is now conceivable, and one can imagine creating structures much larger than the printer itself. The problems here will be in feeding the material to the processing "head", and in controlling the geometry as a convenient fixed reference point is not available as it is in a traditional printer. This should prove a fascinating materials processing and spatial control problem for those who choose to attack it.

10^{all}m Matter compilers and DE-compilers.

In Neil Stephensons's science fiction classic "The Diamond Age", he describes a household device similar to a microwave oven simply called the MC, which we can only assume stands for the Matter Compiler. As well as digital pipelines into people's homes for the delivery of bits are physical pipelines for the delivery of atoms. The MC takes the streams of atoms and converts them to those objects that the consumer desires. This is the appealing ideal of the ultimate printer, a universal machine for manufacturing everything we need, when we need it. A science fiction fantasy, it does however appeal to our desire for manufactured things. Of course, a matter compiler will require a matter decompiler or we will quickly find ourselves buried by the objects of our desire. Again, nature offers us the inspiration for an elegant solution: planned obsolescence. The key difference between nature's planned obsolescence and the planned obsolescence so often ridiculed in human engineering, is that nature implements a most efficient recycling system. This biodegradation is a most noble goal that humans too must plan for in our printers and manufactured goods of the future.

Ultimately we are interested in building with systems that span the greatest range of scales and materials. The elegant complexity of

natural systems comes from a deep hierarchy of self-assembling components - even the humblest of trees have nanometre scale devices for routing water flow that enables them to build metre scale objects. If we aim to build macroscopic 'things' that have a similar functional complexity (logic, actuation, chemically active surfaces etc.) then we will need to arrange material at the sub-micron scale through to the mm scale and beyond. To that end, this thesis works at patterning functional materials at the micron scale, quickly, and in three dimensions, such that similar levels of heirarchy can be imitated inorganically.

3 – PEMS: Printed Electro-Mechanical Systems

The as stated goal of this work is to produce a printer and suite of printable materials capable of printing electronically active structures and mechanically active structures and ultimately to combine the two. Where rapid-prototyping at the macro scale has greatly assisted prototyping and product development, no similar tools have been developed to viability in the growing field of micro-electro-mechanical-systems, or MEMS. In good part this is due to the fact that mere reproductions of physical structure that can be used for flow modelling, or aesthetic or ergonomic design iteration in macro structures do not offer a useful tool to engineers concerned with MEMS. At the micron scale of MEMS we are primarily interested in the mechanical, chemical, and electrical characteristics of nearly invisible designs. As such a rapid-prototyper or printer at the micron scale by necessity needs to build in functional materials. To date the processes for 3D fabrication at this scale principally focus on photopolymers with their inherently limited material properties.

MEMS holds the promise of opening up a large number of applications in interesting domains from the now ubiquitous accelerometers for air-bag triggers and micromirror arrays for displays, to highly creative applications such as direct in-vitro neural recording of insects[20]. My personal interest, and I would argue one of the most compelling reasons to invent modes for faster design iteration time and more various materials, is in the field of artificial life. Typically artificial life has been limited to computer simulations, and to isolated, or at best tens, of robots. To fully explore this realm that is so inspiringly introduced by Steven Levy[21], the capacity to quickly produce many, computationally and physically able mechanisms would hasten the evolutionary (a combination of Lamarckian and Darwinian) cycle of these mechanisms. Emergent

behaviour of individuals and groups could be realistically studied in a physical sense, not limited to computer simulation. A MEMS rapid prototype tool is necessary for the exploration of swarms of micromachines.

Current state of the art.

Electronic and electromechanical components are presently fabricated in large, immobile manufacturing facilities that are tremendously expensive to build and operate. For example, semiconductor device fabrication generally requires specialized microlithography and chemical etching equipment, as well as extensive measures to avoid process contamination.

The large up-front investment required for manufacturing capacity not only limits its general availability, but also increases the cost of custom fabrication. For a small custom order to be financially competitive with mass production of an established device, the per-unit cost will necessarily be quite high—often out of reach for many designers. Currently, the economics of device fabrication disfavors sophistication and small batch sizes.

In addition to their expense, the fabrication processes ordinarily employed to create electronic and electromechanical components involve harsh conditions such as high temperatures and/or caustic chemicals, limiting the ability to integrate their manufacture with that of functionally related but environmentally sensitive elements. For example, the high temperatures used in silicon processing are incompatible with heat-sensitive materials such as organic and biological molecules. High temperatures also preclude fabrication on substrates such as conventional flexible plastics, which offer widespread availability and low cost.

These fabrication processes are also principally subtractive, depositing a desired material over an entire substrate before

removing it from undesired locations through techniques such as etching and lift-off. Subtractive processes are wasteful; introduce dangerous, costly, and environmentally unfriendly chemicals to the fabrication process; and limit the range of manufacturable devices since the etch chemistry can interact with previously deposited layers. Such processes may also prevent three-dimensional fabrication and large-area fabrication: costly and difficult chemical and mechanical polishing steps are required as planarizing steps in the manufacture of multi-layered devices and, indeed, place some limits on the number of layers.

MEMS processes have traditionally been limited to the techniques of bulk micromachining, surface micromachining, wafer bonding, LIGA, and their combinations and variations[22]. Whilst allowing many wonderful and varied devices, structures derived from these processes are limited in two significant ways; geometric flexibility and material flexibility. Geometries are generally limited to planar geometries and their extrusions with some limited relief due to layer stacking. Materials are basically limited to silicon-based materials for the silicon-based processes, and metals for the LIGA process.

Alternative Routes to MEMS prototyping and manufacture

Decomposition of organometallics

Makino and Shibata[23] reported the laser decomposition of spun coat palladium acetate films to form 50 μm palladium features on glass and polyimide substrates. Thermal conduction limited line widths to 100-200% of the laser beam spot size and features with a fine polycrystalline grain size up to 100nm and a low resistivity on order of $10^{-5}\Omega$cm compared to $1.08\times10^{-5}\Omega$cm for bulk palladium. Trace carbon and oxygen were present in the patterned features consistent with incomplete decomposition of the organic material whilst smaller grain size was present at line edges compared to the centres due to the gaussian beam profile and scanned line effect.

Irradiation densities on order of $6kWcm^{-2}$ at $125\mu s^{-1}$ were required and features showed a relatively flat profile at around 12% thickness of the spun film.

Direct laser based processing.

Direct laser ablation and laser assisted etching of silicon are other well documented processes for micromachining[24]. In silicon etching, the substrate is heated locally to the melting point whence the surface is rapidly etched by molecular chlorine. Laser assisted etching to 0.5μm feature sizes has been reported[24].

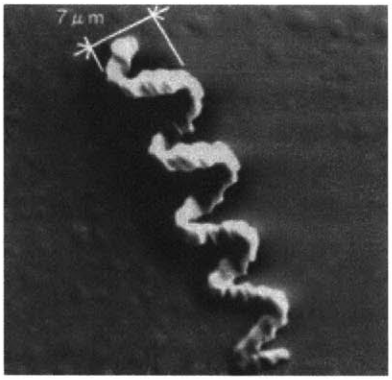

Figure 3.1. SEM image from Maruo and Kawata[25] of micro-coil in photopolymerizable resin by two photon absorption technique. Reported resolution of 0.62μm laterally and 2.2μm in depth.

Two Photon techniques[25] utilise the quadratic dependence of the two-photon absorption rate on light intensity to confine absorption to the highly localized area at the focal point. This makes three-dimensional resolution possible and has also been applied to 3-D memory and 3-D fluorescence microscope imaging. Whereas traditional stereolithogrphy techniques are limited to the minimum thickness of resin layers this process is promising in 3D microstereolithography because the resolution in all dimensions is optically defined. Geometries are however limited to line of sight interference in the optical path unless the refractive indexes of cured and uncured materials are substantially similar. One

drawback of this method is that extremely high energy lasers are required; often several kW.

Photo-Electroforming.

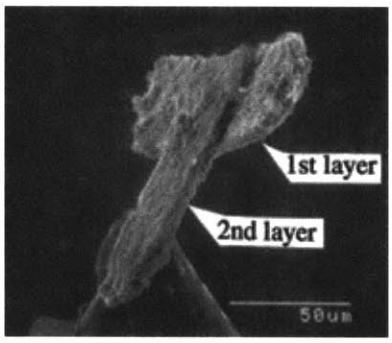

Figure 3.2. Two layer part in Ni/SiC by photo-electroforming by Tsao and Sachs

The photo-electroforming technique of Tsao and Sachs demonstrates a conceptual route to many-layer 3D parts in a large library of materials. The process is similar to a laser sintering process. A bed of porous or powdered material is submerged in an electroplating solution. A high energy laser (Argon Ion) is focused and scanned over the powder and plating is induced from the solution onto the powder at the point of focus. Additional layers can be stacked upon the original layer. 5μm layer thicknesses and 10-15μm planar resolutions were achieved by this method. The range of materials includes many metals and ceramics but is limited to those materials that have a significant absorption in the spectral range within the high transmittance spectra window of the plating solution and those that can tolerate surface temperatures of 200-300°C. Surface finish is limited to the particle size of the precursor powder.

Stamping.

Micro-contact printing, and its derivatives, was pioneered by Whitesides and his co-workers at Harvard[14]. This route to device fabrication utilises elastomeric stamps cast from etched silicon or photoresist on silicon master templates. The general principle involved is the casting or transfer of liquid precursor materials onto a substrate in contact with the mold. In work patterning self assembling monolayers (or SAMS) resolution to 35nm has been achieved[14]. A derivative technique termed "nano-embossing" has been successfully developed and utilised in the Nanomedia research group of the MIT Media Laboratory to pattern 250nm devices in silver, gold, and SiO2 from colloidal nanocrystalline precursors. The key difference in this process is that it elimates the need for removing the carrier solvent through the stamp material – a time limiting step.

Folch and Schmidt[26] highlight the inherent dificulties of registration by microstamping techniques due to the elasticity of the patterning substrate. They report 5μm registration over 4 inch wafers, consistent with the registration difficulties encountered within our own group's microstamping efforts. Although techniques have been proposed to overcome this limitation, they are yet to be proven. Bubble formation and difficulties depositing large planar features are the other reported limitations with this technique in its current state of engineering.

Ultimately I believe these difficulties will be overcome and this form of printing will be utilised as a low cost high volume production technique to printed electronics. In terms of rapid prototyping it does however face similar limitations to traditional lithography in the requirement for a master patterned from a photomask for each layer employed. Many layered devices will then be slow and expensive to manufacture.

Ink Jet

Although not a serious contender in high quality, high resolution MEMS, ink jet technologies as previously outlined in chapter 2 and Fuller[16] offer very low cost and rapid development of structures with 20 micron and larger resolution. Thermal actuators, radio frequency tags, and electrostatic drive motors have been demonstrated with this technology[16]. The nanoparticulate route in particular offers a realistic paradigm for the employment of multiple functional materials in a single ink-jetting system. Already it is possible to print an electrically conducting metal and insulating layers using this technique to create, for example, three layered, linear electrostatic drive motors.

Electroplating

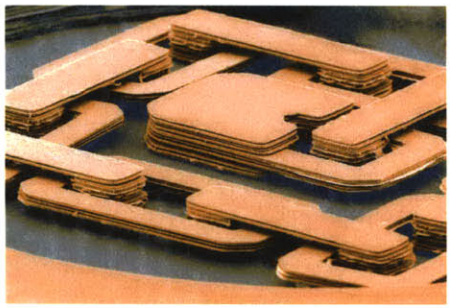

Figure 3.3. Micro chain by 'efab' technique.

"EFAB" is a technique developed at the University of Southern California that uses patterned electroplating deposition to build three dimensional structures[27]. The technique shows perhaps the highest part complexity of any rapid prototyping technique to date at the micron scale, including a 20 layered linked chain structure. The layer thickness is between 5 μm and 20um. The materials for construction are limited to those that can be electroplated. The process also limits the structures to a single homogeneous material. A planarization step is required after each layer in this process - this places a limit on processing time. Typical EFAB devices are constructed in Nickel. Lateral resolution is limited to the mask used

for the photoresist which becomes a liftoff mask for the electroplating process. Because high resolution glass or quartz masks are slow and expensive to produce, high resolution laser printed masks with 5um resolution are employed - this 5um is the lateral limit. There is no obvious route to incorporating functional logic (ie semiconductors) in devices made by this technique.

Summary.

Outlined above are the main non-silicon / photolithography based routes to MEMS devices. Some offer the possibility of flexible rapid prototyping, but at low resolution (ink-jet), or with very limited materials (two-photon absorption of photopolymers), others such as microstamping are more suited to high volume manufacture should the issues of allignment, vias, and multi-layers, be resolved. There is still an obviously unfilled niche in the true rapid prototyping of two and three dimensional structures in functional materials at the micron and sub-micron scale, particularly if logic elements can be included. The author is unaware of a precedent for rapid multiple material fabrication in single devices at the micron scale.

4 - Working with nanoparticles

Melting point depression

Melting point depression in nanoparticles has been known since the discussion of Buffat and Borel[28]. This behaviour was demonstrated in the II-VI semiconductor CdS in 1991 and since considered a general characteristic of nanoparticles regardless of the material system[29]. This behaviour has recently been observed in silicon[30].

The recently published exception to this characteristic is Tin, where for 10 to 30 atom clusters, the melting point is 50K above the melting point of the bulk solid. This is thought to be due to the very different atomic structure of the clusters compared to the bulk element[42].

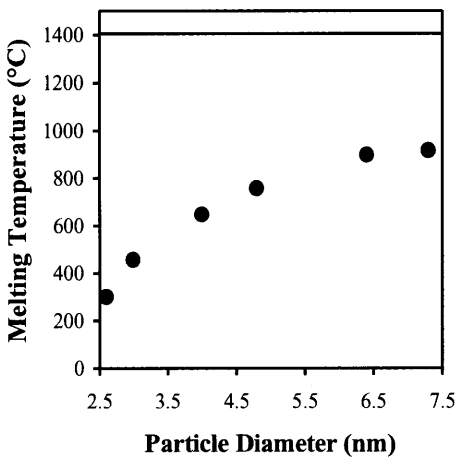

Figure 4.1. *Size dependence of the melting point in the II-VI semiconductor CdS. Alivisatos and coworkers.*[(Gol92)] *The upper line denotes the melting point of the bulk material (1405 °C).*

The size dependence of melting point depression can be seen in the II-VI semiconductor CdS in figure 4.1 (After Alivasatos et.al[31]). The melting point of the particle is close to inversely proportional to the radius. This leads to the sharp decrease in melting point below 5nm. For both gold and CdS nanoparticles, melting points around 300 °C are exhibited at a particle radius of 2.5nm. This is compared to their bulk temperatures of 1063 and 1405 °C respectively.

Zeng et.al.[32] found in simulation studies of nanocrystals that traditional sintering modes are not valid. Only two of the six classical matter transport mechanisms are observed at this scale. The two, surface diffusion, and grain boundary diffusion, are also considerably accelerated. Three additional mechanisms are also observed in sintering systems at this scale: mechanical rotation, plastic deformation via dislocation generation and transmission, and amorphisation of sub-critical grains.

Low temperature sintering at a depressed temperature is also observed prior to melting. This can lead to fine-grained polycrystalline films with grain sizes of the order of the nanocrystals originally deposited[29]. This sintering is believed to occur due to the surface of the particle melting prior to the core. This fuses the particles together and hence melting to the core may never occur as the effective size and hence melting point quickly climbs the steep melting curve of fig.4.1. Studies have demonstrated a reduced temperature for the fusing of particles at approximately 2/3 of their reduced melting point[30].

Ercolessi et al[33] showed using molecular dynamics calculations that for gold clusters a critical size exists for sintering or pre-melting effects. Below a cluster size of 250 atoms, the entire particle melts at once. Above this size, liquid patches develop at the surface of the particle and spread into the core, melting it quickly. As Ridley[34] expressed it, "the absence of pre-melting effects at small sizes is important because it suggests that complete melting and subsequent grain growth is possible. Even with surface melting, a rapid thermal or laser treatment could melt the particle throughout, allowing grain growth beyond the dimensions of the nanoparticle". This is particularly important in the context of printed nanocrystal based transistors, as grain size is a key limitation to electron mobility.

Depositing colloidal solutions

For the printing of logic and MEMS from nanocrystalline precursors, thin wet films of colloidal solutions are required. There are a number of techniques available for the deposition of such films:

Solution casting
Spin coating
Draw down bar
Langmuir blodgett techniques
Dip coating

Solution casting is useful, but primarily as a laboratory technique as control in a manufacturing environment is limited. Spin coating is wasteful, but highly characterised and used industrially in traditional semiconductor fabrication facilities. The draw down bar method is similar to drawn bar methods used in traditional printing processes. Within our laboratory we have drawn films to thicknesses on the order of a micrometer and by controlling the concentration of the nanocrystals in solution have been able to further reduce the thickness of a solid film to ~100nm after solvent evaporation. Langmuir blodgett films are of limited application in this area and are more typically used where atomic monolayers are desirable. Dip coating techniques can also be wasteful and not surface specific and it is difficult to imagine their role in the printing routes described herein.

The continuity of the as deposited films is crucial to obtaining reliable device performance. In semiconductor devices the thickness of the deposited films can be controlled to determine the off current for the device. Thinner layers decrease the off current.

Ridley[34] describes also how the mode of deposition may also effect device performance in semiconductor films. The self assembly of deposited nanoparticles into hexagonal close packed arrays is

observed in some nanocrystal systems when the solvent/cap evaporates slowly enough to allow the nanoparticles to find lattice sites as they fall out of the suspension. Such "superlattices" have been formed with grain sizes as large as 50μm by carefully evaporating appropriate solvent mixtures.

Lange[35], offers an excellent review of solution routes to single-crystal and polycrystalline thin films. Spun coat or dip coat films on single crystalline substrates can be induced to grow epitaxially. On evaporation of carrier solvents, a solid precursor film forms that decomposes to a polycrystalline film during heating. Further heating can induce epitaxial growth to single crystal films. Lange's work focuses on metal organic, metal salt, polymeric and carboxylate precursors to be pyrolyzed to synthesize oxides, carbides, nitrides and a limited number of pure metals. Of most relevance to this work, Lange illustrates that the large volume decrease on evaporation and pyrolysis can lead to 'mud' cracks where the film thickness is greater than a critical value. These mud cracks form due to biaxial stresses induced by the volume change in the film. A critical film thickness can be determined below which cracks are avoided. If Griffith crack growth criteria are used (ie. A crack can only extend if doing so reduces the free energy of the system) a critical thickness can be determined for different materials. For most brittle gels this is around 100nm. In a layered micro-building process, and for creating crack free insulating films for logic applications, this provides an insightful route.

Little work has been done characterising the mechanical properties of thin films formed from nanocrystalline precursors. Some researchers have however formed semiconductor thin films from nanocrystalline precursors, principally for application to photovoltaics. CdS and CdTe are the main materials in these studies which utilise clusters from 30nm to less than 1nm in size. Fusion

temperatures between 200 and 550 degrees celsius have been observed for the particles in these studies.

Thin Film Properties - Grain size

Grain growth in thin films derived from nanoparticules has been best studied in the fabrication of solar cells[36]. CdTe colloids were spray deposited onto hot substrates. Grains 6 to 30 nm in size were formed from 2.5 to 7.5nm diameter nanoparticles at 400°C deposition temperatures. There is no residual nanocrystalline topography in these films. Most importantly these films have been used in the fabrication of high-quality CdTe solar cells, with the best reported cells having an active area efficiency of 10.5%[36].

A similar spray-deposition approach has been used to form pure CIGS films, again for solar cell fabrication. 10 to 30 nm amorphous nanoparticles were deposited at 550 °C and formed porous films. Grain growth was observed, but researchers did not comment on the size of the grains. The best film exhibited a conversion efficiency of 4.6%.

Why this material system?

Building anything requires three things: materials processing, information input, and materials transport. In any rapid prototyping system one needs to consider all of these processes. Information input is now achieved routinely with a PC and the heart of the problem in new systems is appropriate choice of the material transport and processing mechanisms.

In a rapid prototyping tool one is concerned with the build speed. This relates to the processing parameters for the material system employed. Nanoparticulate systems offer distinct processing advantages in lowering the processing temperatures (even by

photonic curing it is a thermal process) to temperatures below 300°C. Lower processing temperatures mean less time lost in heating and thermal dissipation.

A fluid offers greatest advantage in materials transport ease, which is obvious if we consider that all 'living' organisms use liquid based materials because the pumping and transport is simplified.

Temperature is particularly important in building a multi-material printing system that includes semiconductors and metals, as inter material diffusion is limited at these low temperatures. Processing temperatures in this range also allow for a mixed material system that includes metals, semi-conductors, and polymers - conceptually enough components to build functional logic.

The reason for considering a nanoparticulate system for rapid prototyping is that it offers a large material library, all in a convenient liquid form, with low temperature processing capability. It should not be surprising that this is a good theme for building a large variety of structures from minimum components, as life uses fluid based precursors and a basic set of amino acids which can all be processed close to ambient temperatures to build an enormous array of things.

There are however disadvantages to this system. The nanocrystalline colloids employed require a stabilizing surface group to prevent premature agglomeration of the highly reactive crystals. These organic groups (typically a thiol) have a lower boiling point than the melting point of the inorganic component, however in a three dimensional film it is not always possible to remove the organic groups entirely and carbon and sulfur impurities can remain. Again, particularly in the context of printing high mobility semiconductors that require high purity, this is problematic. The highly reactive particles also tend to agglomerate over time, and the properties

and processing parameters change deleterious with aging precursors.

In general , nanoparticulate material systems can be seen to have distinct advantages in enabling multiple material, functional, 3D fabrication tools. Their expense lends them to the micron scale domain at present, however the solution based synthesis routes potentially offer low cost sources. The remainder of this thesis examines their performance in a number of test fabrication schemes.

5 - Nanoparticles and Energetic beams

Serial scanning of IR diode laser

Recognising that thermal energy could transform nanoparticulate precursors into solid thin films, a program of utilising an IR diode laser on an XYZ gantry to cure spin cast films of nanoparticles was embarked upon. The processing scheme for building devices by this route is shown in figure 5.1.

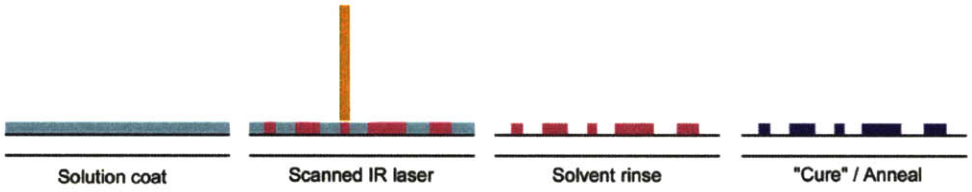

Figure 5.1. Process scheme for scanned selective laser curing.

Figure 5.2. shows the IR absorption spectra for a Ag nanocrystalline colloid indicating strong absoprtion peaks at ~1000, 3000, and 3400nm. A 1064nm IR laser was chosen as the radiation source based on this data. It should be noted that the absorption peaks can be tuned by controlling the size of the nanoparticles and does not limit this process to the IR.

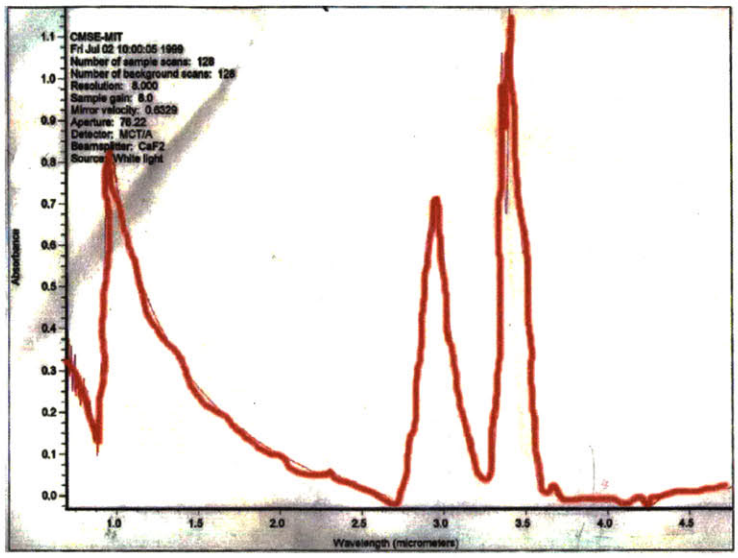

Figure 5.2. IR Absorption Spectra for Ag nanocrystalline colloid.

Experimental

A 5W Ytterbium Fiber Laser (YLD-5000) by IRE Polus was employed. The laser emits coherent, collimated light at 1064nm. Standard microscope objectives were used to reduce the beam to a diffraction limited spot size. The laser and lens assembly and an electro-mechanical shutter were mounted to an XYZ positioning system by Aerotech. The X,Y,and Z positions, the laser power, and the shutter operation were controlled using a modified G-code scripting language run on a PC.

Thin films of nanocrystalline material were prepared by spin coating a suspension of nanocrystals (30% Ag by weight, in α-Terpinol) on to substrates. The heavy alcohol carrier was removed by pulling vacuum around the samples in a bell jar. Typically substrates were 1x3" laboratory grade clean glass slides, though silicon wafers and polyimide (Kapton) films were also used. After vacuum assisted solvent evaporation a thin "green" film of thiol capped nanocrystals remained on the substrate. The film thickness was varied by changing the spin speed and solvent concentration.

Laser power was varied to compensate for changing writing speeds, lens configurations (spot size) and film thickness. Fluences of 80 Jcm^{-2} are sufficient for complete conversion to a metallic film from a green precursor for 150nm thick films. Variations in film thickness greatly affected results due to differing absorption.

After laser curing slides were rinsed in a solvent (typically hexanes) to remove uncured material. A post curing anneal at 250°C on a hotplate was performed.

Results

Conducting lines 2um in width and up to 50 mm in length were created. Conductivity was measured according to $\rho=RhW/L$ where R = resistance, h = height, W = width, and L = length. and was

typically of the order of 5 x 10^{-5} Ωcm^{-1} compared to the reference value of 1.589 x 10^{-6} Ωcm^{-1} for bulk silver. Figure 5.3a) shows a typical contact pad and line as used for conductivity measurements. 5.3b) and c) show over-exposed and correctly exposed lines respectively. The over-exposed lines cause a melting effect in the centre of the line which is explained in the next section.

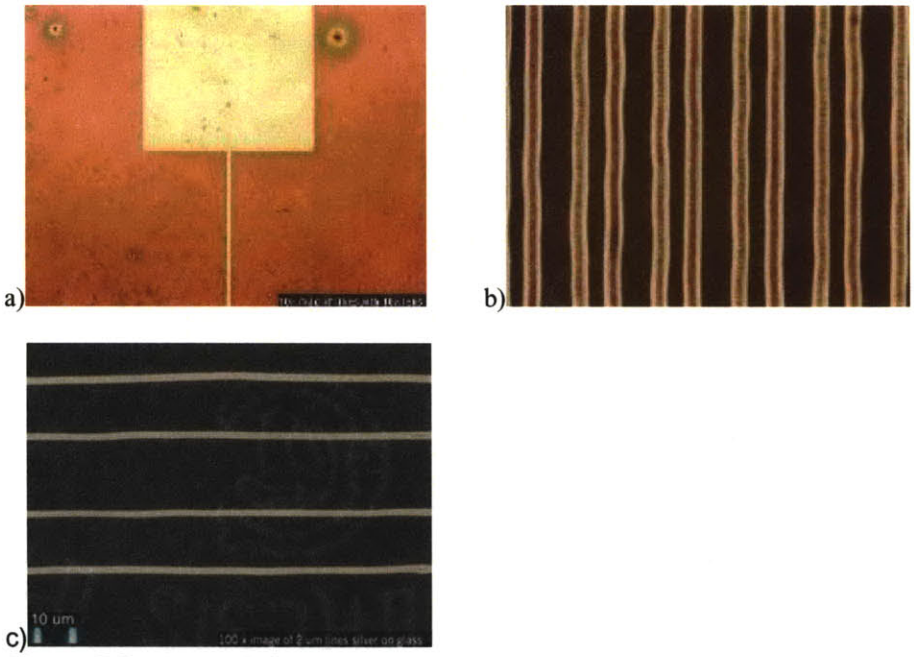

Figure 5.3 a,b,c. a) Contact pad and line for conductivity measurements. (unwashed slide) b) 6μm lines demonstrating effect of gaussian beam distribution. c) 100x magnification image of 2μm lines on a glass slide.

Gaussian Beam Effects and line morphology.

The gaussian beam profile of the IR laser proved a limitation of this process. This effect is compounded by the planar cross section of the beam. Because it is circular, the centre of any scanned line receives a higher energy flux for any given scan rate. As can be seen by the images in figure 5.4, at the extremeties of the beam where a lower energy flux is present, the nanocrystalline precursor is seen to have sintered to a fine crystalline solid. In the centre of the beam the nanocrystalline silver has heated to the bulk melting point and flowed into droplets on the poorly wetting glass surface.

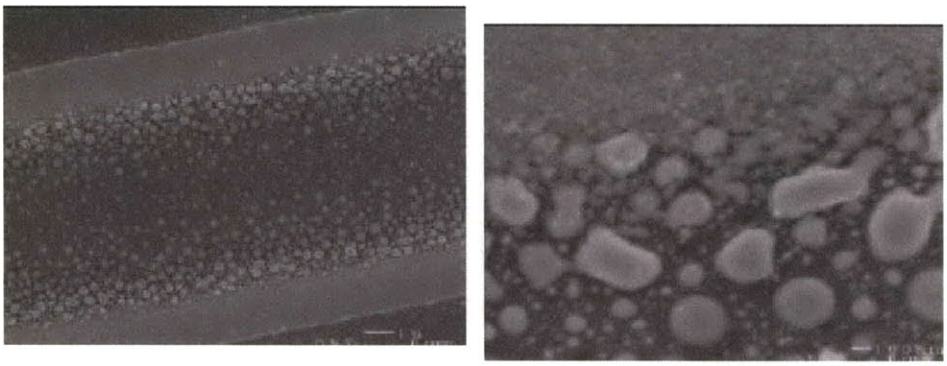

Figure 5.4. SEM of cured line at low and high magnifications demonstrating the effect of a roughly Gaussian energy distribution within the exposing beam. The Outer edges of the line are cured whilst the centre has melted and flowed into 'islands'.

In the optical micrograph of figure 5.5, the heat affected zone around the cured line is easily visible. In this case, the centre of the line is cured appropriately, though at the edges of the line a semi-cured zone is apparent with a noticeably thinner 'green' film beyond that. This thinner film is likely due to mass loss associated with boiling off of residual solvent groups.

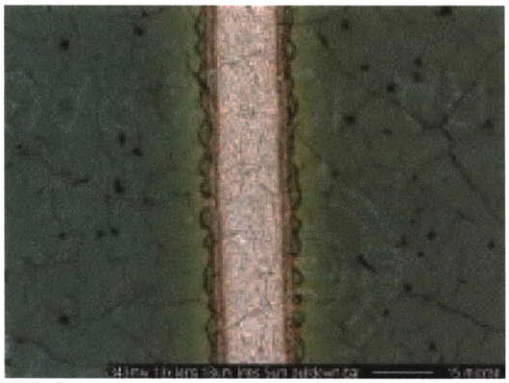

Figure 5.5. Heat affected zone around a cured line.

Multiple layers.

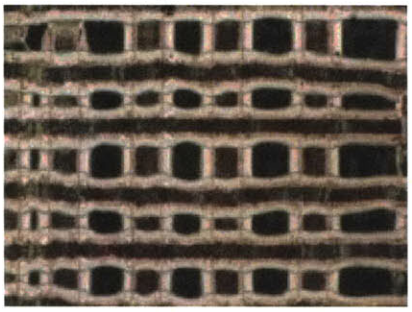

Figure 5.6. Optical micrograph of multiple layer device.

Figure 5.6. demonstrates a crude three dimensional structure written in two subsequent layers. Without a releasable support material, the second layer assumes the topography of the first. The lines in figure 5.6 exhibit significant melting in the centres.

Serial limitations.

The serial nature of a scanned beam process such as this means fundamentally slow processing. Figure 5.7. shows the fill pattern associated with printing large areas via a scanned line. This was the motivation for moving to a parallel processing technique based on light modulation by a micromirror array.

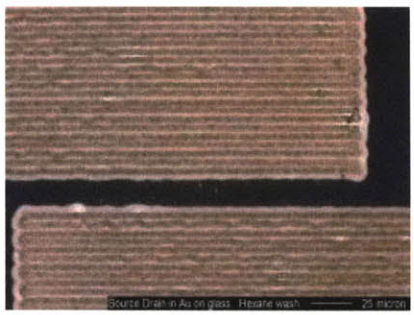

Figure 5.7. Optical micrograph of serially patterned source / drain electrode structure showing fill pattern.

Thermal vs. photo-cleavage curing.

To determine the nature of the curing process a simple experiment was devised. The principle question is whether the material cures due to thermal processes: light absorption leading to heating and

removal of capping group with subsequent sintering of nanocrystalline film, or whether a photo-cleaving process is involved: ie that the process is due to photon induced bond scission.

Two samples were exposed to the laser for the same cumulative period, absorbing the same cumulative energy flux. In the first sample the exposure was continuous. In the second sample, the exposure was divided into shorter units with a timed interval between units to allow for thermal dissipation. In a purely thermal exposure process one would expect the first sample to convert to metallic silver from the nanoparticulate precursor, and in the second sample not to. This is in fact what was observed. In the second sample receiving the same total flux of 50 J/cm^2, at a duty cycle of 20 (on:off = 1:20), no curing was seen.

Through mask patterning utilising broadband UV

Through mask patterning with UV was briefly explored as a mode to printing large area metallic patterns directly from a photomask without the use of photo-resists, vapour deposition techniques, and traditional processing. The simple processing scheme for such a method is outlined in figure 5.8.

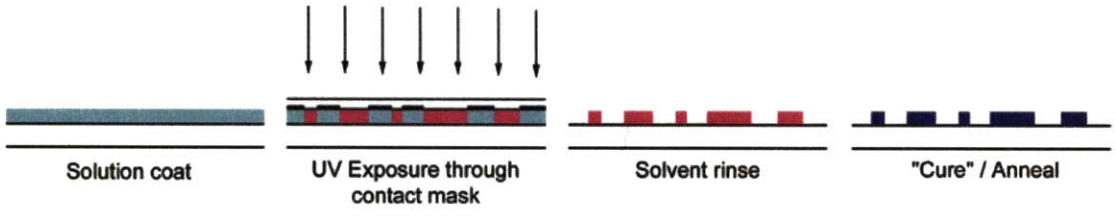

Figure 5.8. Processing scheme for UV patterning through a mask.

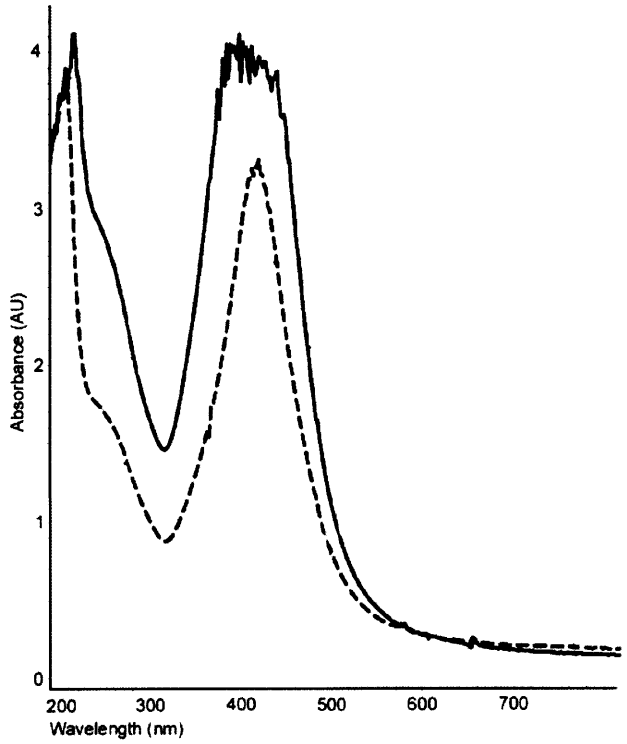

Figure 5.9. UV - Vis absorption spectra of nanocrystalline silver.

Experimental

An EFOS ultracure 100ss UV light source projected UV through a traditional chrome on quartz photomask. Thin films of nanocrystals on glass slides were prepared by spin coating. A solution of 30% Ag nanocrystals in α-Terpinol was diluted with chloroform to obtain a 3% by weight solution of Ag nanocrystals in chloroform. This low boiling point solvent alleviates the need for vacuum assisted solvent removal post spin coating. Film thicknesses for a 3% weight solution spun at 2500rpm for 30s were typically 150nm as measured by a 'scratch and AFM' method. This thickness could be varied by changing the spin speed, or the weight percent, of Ag in the spun solution.

The minimum linewidth is defined by the features of the contact mask. In this work 5um lines were the smallest produced, as defined by the smallest available mask pattern. Typical results can be seen in figure 5.10.

The curing process in this technique differs slightly from that described for the laser curing above. A "semi-curing" of the nanoparticulate precursors was observed. After exposure to UV (typically 2 Wcm^{-2} for 180 seconds) a noticeable colour change of the precursor film was observed. In this state the film did not appear metallic in colour, nor did it conduct current. The semi-cured state survived a hexane wash after which it was thermally cured on a hot plate for 90s at 250°C. It is thought that this semi-cured state is achieved when the bulk of the organic solvent and capping groups have been removed, but the nanocrystals have not been raised to a sufficient temperature for significant sintering to occur.

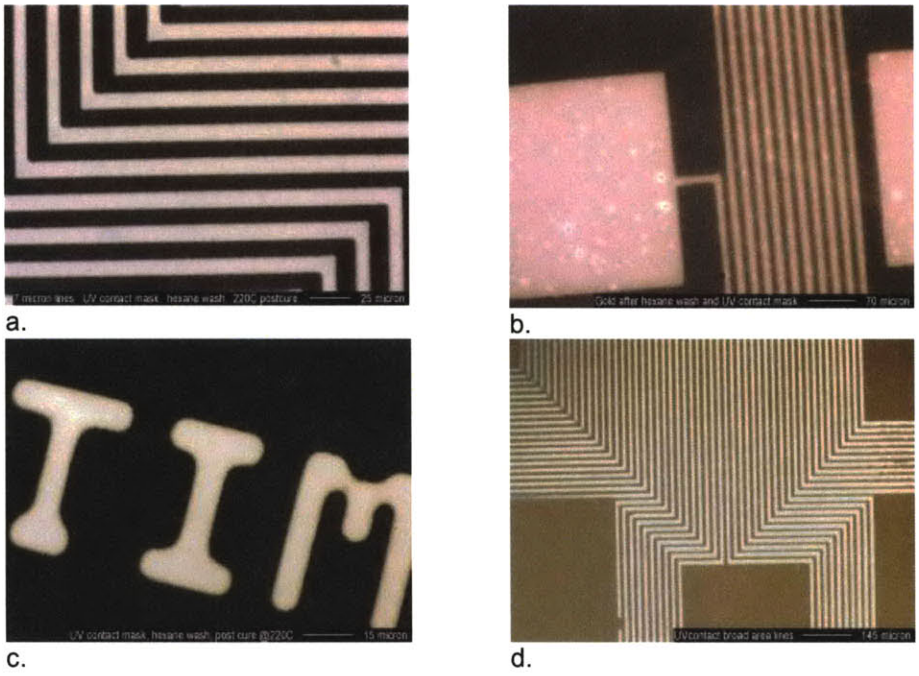

Figure 5.10. Patterned metals on glass. a.) 5 micron silver lines. b.) 7 micron gold lines. c.) 5 micron features in silver. d.) Large area printing in a single exposure.

Conductivities of 7.5 x 10^{-5} Ωcm^{-1} were measured for lines 250 microns in length and 5 microns wide. As would be expected, this is similar to the conductivity measured for laser cured and e-beam cured lines in this work as a post cure anneal is used in all cases. The conductivity

is a general property of the nanocrystalline precursor, with small differences due to the level of impurities remaining after processing.

Electron Beam Lithography

Background

With lithography and micropatterning of materials, one is always interested in the ultimate resolution. To this aim electron beam lithography of the nanoparticulate colloids explored in the above techniques were tested as precursors for direct electron beam writing of metallic structures.

Previously, Clarke et.al. utilised electron beams to fuse organometallic gold clusters ($Au_{55}(P(C_6H_5)_3)_{12}Cl_6$) to a Si_3N_4 coated Si wafer. Electron beam doses were below the level required to remove the stabilising thiols such that the group could test the electron tunnelling characteristics. These devices were successfully tested as coulomb blockades[37]. The direct writing of gold nanostructures to 150nm linewidths has also been reported by focused ion beam lithography using metalorganics[38].

The use of organometallics as precursors for metallic lines is well reported including[39], however the large ratio of organic to metallic material is problematic in defining impurity free devices. Typically organometallics have a ratio of 10:1 organic to metallic material. More recently surfactant stabilised nanoclusters have been of interest due to the higher metallic content (closer to 1:1 for 6nm metal nanoparticles passivated by $C_8H_{17}S$ [40]).

Reetz et.al[41] used $(C_8H_{17})_4N^+Br^-$ stabilized 2.0nm Pd clusters (69% metal content) to define linewidths to 30nm on GaAs substrates. The 2nm clusters were shown to agglomerate to 4-5nm under the influence of the electron beam and grow further to 8-10nm on a post anneal. Typical dosages of 200 000$\mu C/cm^2$ were used for 50nm linewidths. Resistivities of 1928.5$\mu\Omega$cm and 181$\mu\Omega$cm were measured for post e-

beam and post anneal samples respectively. These are 2 orders and 1 order of magnitude higher than bulk Pd indicating carbonaceous residue.

Bedson et al[40] patterned $C_{16}H_{33}S$ passivated 4nm gold clusters on highly oriented pyrolitic graphite substrates to define features as fine as 26nm with spacing of 30nm using an electron beam to remove the passivating ligand. No conductivity data was given, and EDX of the resulting structures showed a low gold content potentially indicating high carbon contamination. No dosage data was recorded.

This work

Direct electron beam writing of three dimensional nanostructures was explored after the SEM analysis of optically patterned thin films demonstrated that the electron beam was changing the nature of the film during observation. The observed e-beam/film interactions of thiol-capped Ag and Au nanocrystals resembled the volatilisation of the capping group observed in[40,41].

The processing route used is as outlined in figure 5.11. Solution coating was achieved via spin casting of nanocrystalline solutions. Electron beam scanning was performed under computer control of e-beam optics with field stitching. Solvent rinse was with hexane in two aluminium weighing dishes; 8 second dip in hexane in bath #1; then immediately a 4 second dip in clean hexane bath #2. Wafers were dried with nitrogen gas. Except where otherwise stated, a post exposure anneal was performed for 10 minutes on a 200°C hotplate.

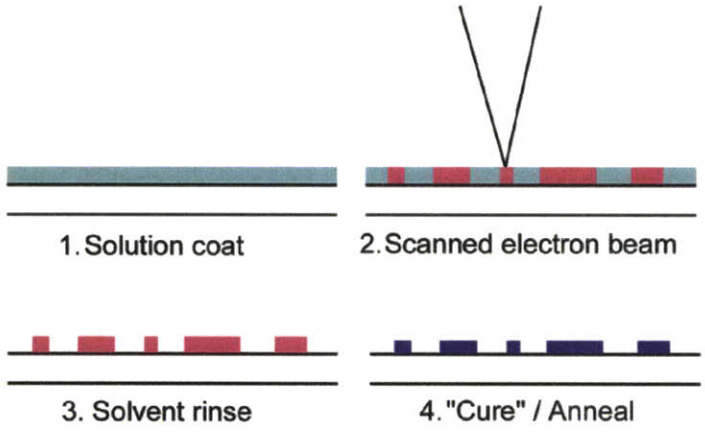

Figure 5.11 Direct electron beam write process route.

Initial exposures of gold and silver nanocrystals (2.5% in Chloroform), on 100nm SiO_2 on highly n-type P doped Silicon wafers were conducted. An exposure matrix test was performed for large area blocks, and small lines. The doses were according to table 5.1.

Feature	Current (pA)	Dose (uC/cm2)	Freq.
400 micron field size			
Num. 1	1,000	330	0.5 Mhz
Num. 2	2,000	660	0.5
Num. 3	3,000	1,000	0.5
Num. 4	3,000	2,000	0.25
Num. 5	3,000	3,000	0.16
Num. 6	3,000	4,000	0.12
Feature	Current	Dose	Freq.
75 micron field size			
Bar 1	65	330	0.95 Mhz
Bar 2	130	660	0.95
Bar 3	200	1,000	0.95
Bar 4	200	2,000	0.48
Bar 5	200	3,000	0.32
Bar 6	200	4,000	0.24

Table 5.1. Dose and current for ebeam exposure matrix.

As might be expected, lighter doses led to subsequently thinner films in the cured product. This can be seen in the optically thinner films of figures 5.12 and 5.13. at lower exposure doses. For doses above 2000 $\mu C/cm^2$ of the larger features, significant exposure due to back

scattered electrons can be seen giving the blurred edges shown in figure 5.13. For finer features, lower doses are insufficient to bind the exposed material to the substrate and lift-off during the solvent wash is exhibited. It was found that ideal exposure doses of 1200 $\mu C/cm^2$ for smaller features, and $800\mu C/cm^2$ for large filled areas for silver films, and $1000\mu C/cm^2$ and $1500\mu C/cm^2$ for gold films was ideal.

Figure 5.12. Test exposure matrix. Exposure conditions as in table 5.1.

Figure 5.13. 50x micrograph of numbers 2, 3, 4, test exposure matrix.

Multiple Layer Fabrication

A program of multiple layer fabrication was undertaken after exposure doses were tested. The processing steps were the same, with subsequent layers spun over the original patterned layers. The simple electron beam stereo lithography process is outlined in figure 5.10 and 5.14. Three wafers were exposed with subsequent layers in 1.) silver, silver, silver, 2.) silver, gold, silver and 3.) gold, gold, gold configurations to test the generic building technique for multiple material functionality.

A three layered test structure can be seen in Figure 5.15. exhibiting misalignment.

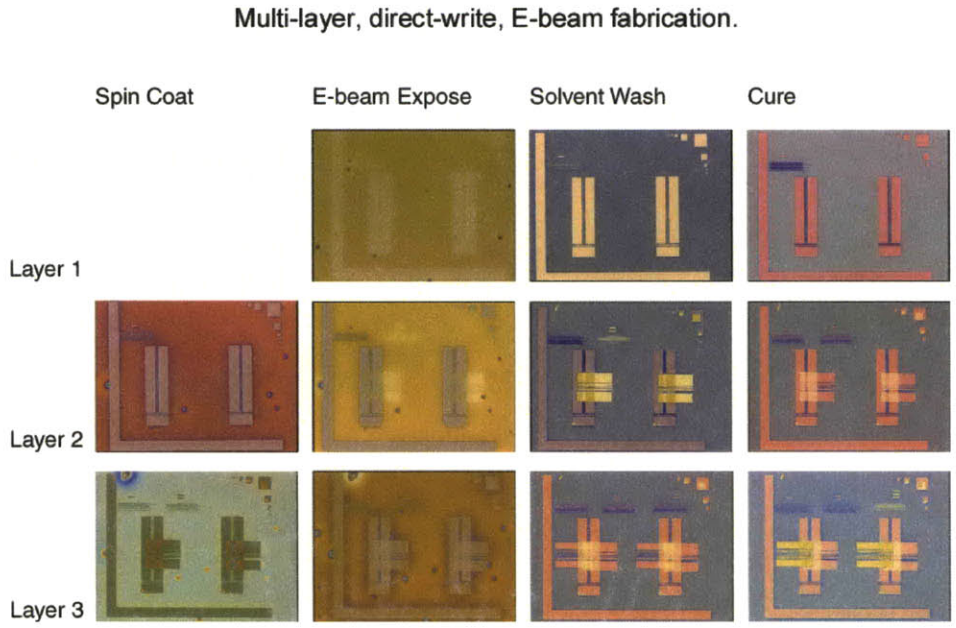

Figure 5.14. Multiple layer fabrication

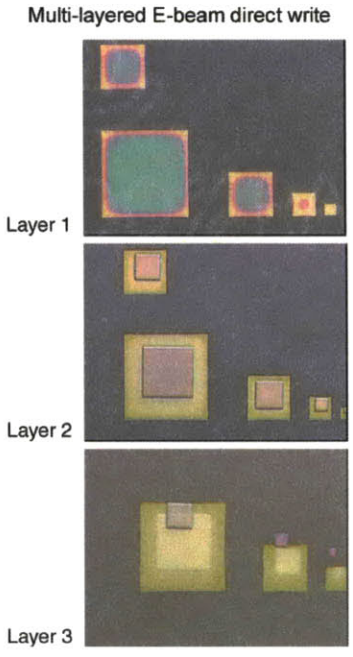

Figure 5.15. Three layered test structure in silver. Misalignment can be seen on the third layer, in this case due to an uncompensated shift in the e-beam optics.

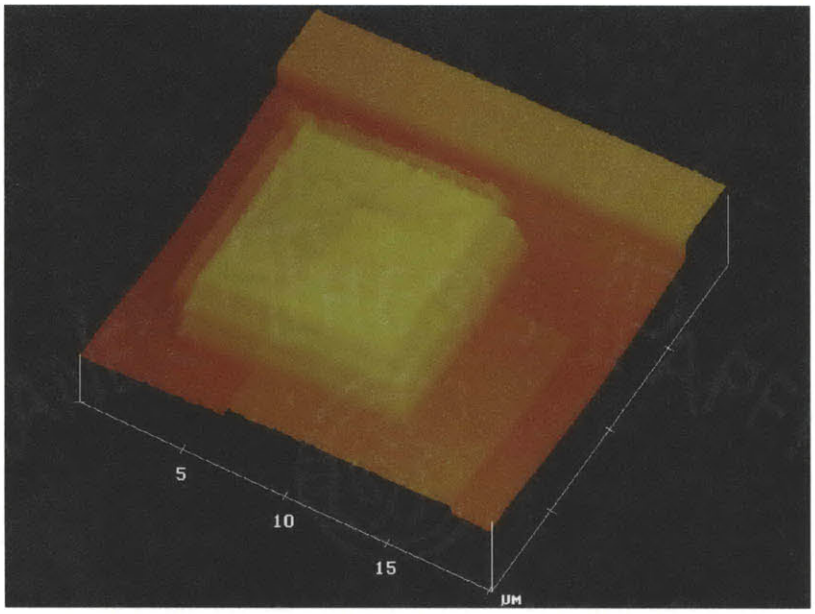

Figure 5.16. Four layers (Au, Ag, Ag, Ag) on Si. Note alignment errors.

Figure 5.16. shows a four layered structure. Because no support material is used, each layer can be seen to conform to the topography of previous layers. Alignment over many layers proves extremely difficult by this process where the stage and sample are removed from the vacuum chamber after each layer. Novel alignment techniques are described later.

Minimum features.

As is always of interest in lithography, the limits of resolution were tested in this build scheme. Single lines were written and imaged with AFM and SEM.

80 - 100nm minimum linewidths were observed, consistent with the 70nm aperture size determining focal limits of the electron beam lithography system employed. Significant linewidth variation is exhibited due to backscattered electron exposure, and the fusing of adjoining nanocrystals. Also seen in the SEM images of figure 5.17, is the spontaneous fusing of 'islands' in the nanocrystalline film postulated as due to the removal of the protecting organic capping group by the high vacuum environment of the E-beam lithography

apparatus. These islands may also be due in part to incomplete removal of uncured material in the solvent wash. Figure 5.18 is an AFM measurement of the minimum linewidth confirming 90nm lines with significant edge roughness.

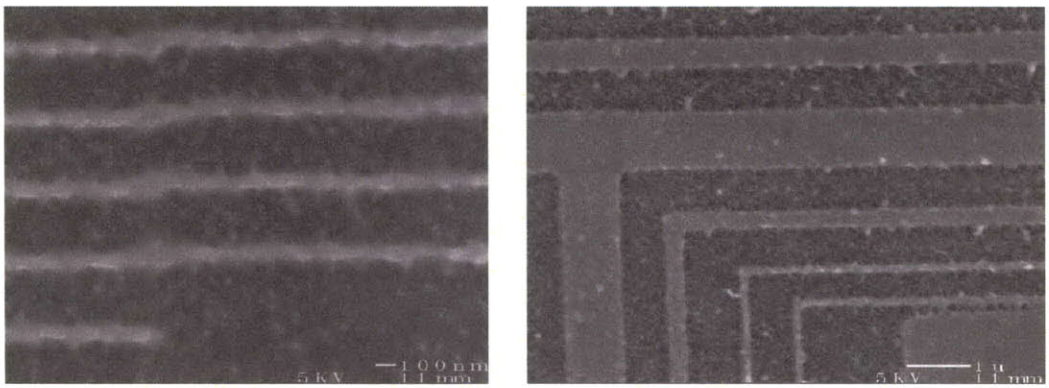

Figure 5.17. Minimum linewidths of 90nm determined by SEM. Significant edge roughness can be seen due to back scattered electron effects, and the fusing of proximal nanocrystals.

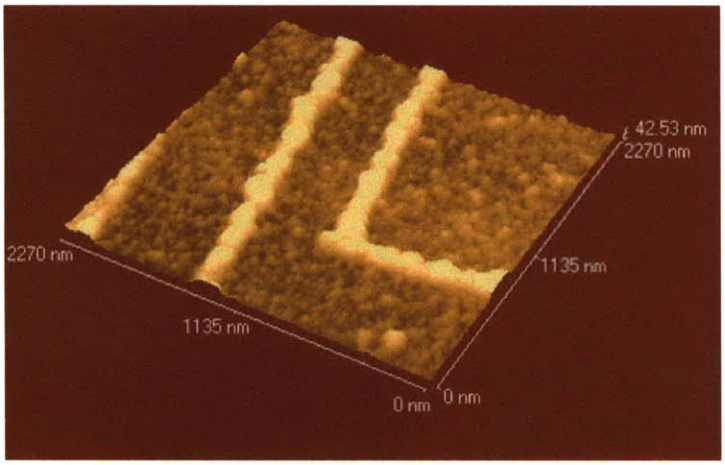

Figure 5.18. AFM measurement of minimum linewidths.

Multiple materials and properties.

The versatility of the process in combining multiple materials was tested successfully by writing successive layers of silver, gold, silver. Each adhered sufficiently to the previous layer to survive the solvent wash. Mechanical properties and interfacial properties were not measured. The conductivity for silver patterned by this technique was measured at $6.7 \times 10^{-5}\ \Omega cm^{-1}$ and $2.0 \times 10^{-5}\ \Omega cm^{-1}$ for gold. Both

values are within one order of magnitude of the bulk element. Measurements were taken of lines 1000 microns in length and 30 microns wide. The above results are conservative as the thickness and width over the entire length of the line was not measured, only at a sample point measured by AFM. The height of the measured lines was 40 and 48 nm respectively for the silver and gold. This height measurement is expected to be the chief source of variation in geometric error.

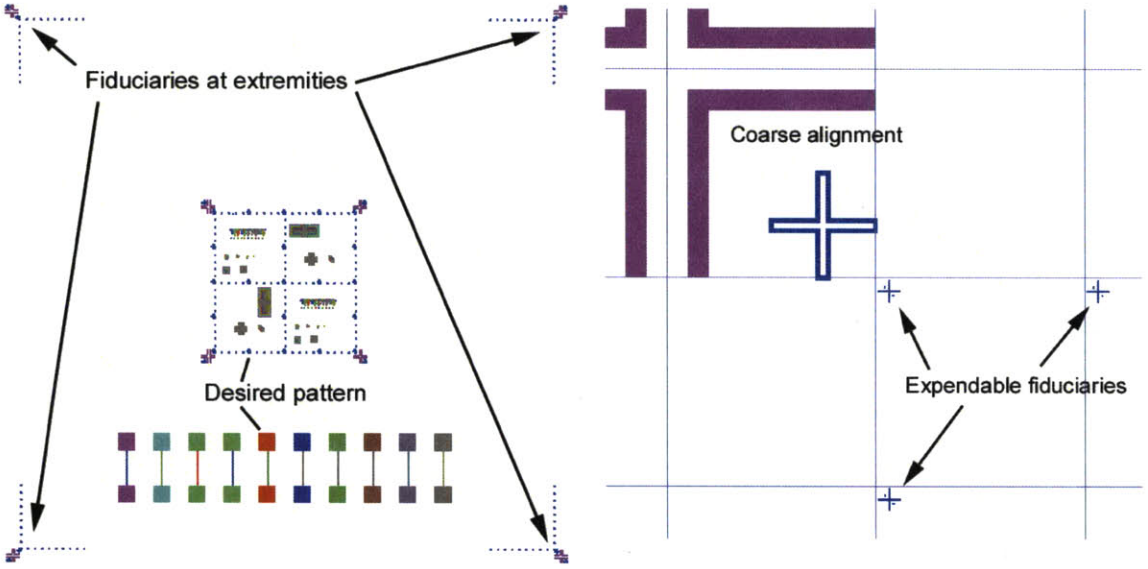

Figure 5.19. a) Fiduciaries can be seen at the four corners of the exposed pattern. b) Close to the coarse alignment features were sets of expendable fiduciary marks. As these fiduciaries are imaged they are exposed and are hence unavailable for imaging in subsequent layers.

Registration techniques.

A novel multi-layer alignment system was developed based on expendable fiduciaries. In the first exposed layer, fiduciary marks were written at the extremities of the four corners of the desired pattern. These included large coarse alignment features, and sub-micron expendable fiduciaries. Between layer exposures, the alignment features were imaged using the SEM function of the exposure apparatus. Because imaging of the fiduciaries at high magnifications itself induced curing of the nanocrystalline film, for the

fine alignment features redundancy of one expendable fiduciary per layer was employed. Mapping of at least two extreme fiduciaries was used to correct the ebeam write system for alignment. Figure 5.19. illustrates the larger scale fiduciaries positioned at the extremeties of the written pattern, and a detail of the expendable fiduciaries located near coarse alignment features.

Conclusions

Three methods for patterning passivated nanocrystalline films are described above; linear selective laser sintering by IR laser, UV contact mask lithography, and electron beam lithography. By virtue of their depressed melting point, nanocrystalline materials can be seen to enable all of the above processes with the advantage of a larger available material library. Each of the methods offers shorter processing time and simplicity over traditional semiconductor photolithography and electron beam lithography techniques. Each also exhibits interesting potential application domains including the potential for micro-stereo-lithography by layering.

The UV patterning technique offers high-throughput processing of patterned metals on arbitrary substrates using traditional photomasks. Although not a truly flexible printing process in the context of giving arbitrary geometry under computer control, a scheme using a single mask defined with the multiple layers of a device and stepping through the features in the mask is possible.

The linear scanning laser technique offers true flexibility, though more work in the optics and laser source is required, and the process will be slow for many multiples of layers.

The electron beam lithography route offers feature sizes to 100nm and potentially below, but the speed of building multi-layered devices in this route is limited greatly by the necessity of a high vacuum and the scanning speed of the laser. Scanning probe

electron beam lithography in the style of Wilder[10,11] is a possible route to non-vacuum multilevel e-beam lithography using these nanocrystalline materials.

6 - A Laser based rapid prototyping tool for MEMS

Following on the early work presented in chapter 5, and retaining the original goal of a rapid prototyping tool for 3 dimensional MEMS, an experimental apparatus was designed and built. An argon ion laser modulated by a micromirror array is the principal patterning technique employed. This system can be used for testing selective laser sintering of nanoparticulate colloids and other thin films and for the photocuring of appropriately sensitized polymers and glasses. This apparatus is also shown to be practical in the rapid manufacture of elastomeric stamps for microcontact printing methods and their derivatives. The experimental apparatus is shown schematically in figure 6.1.

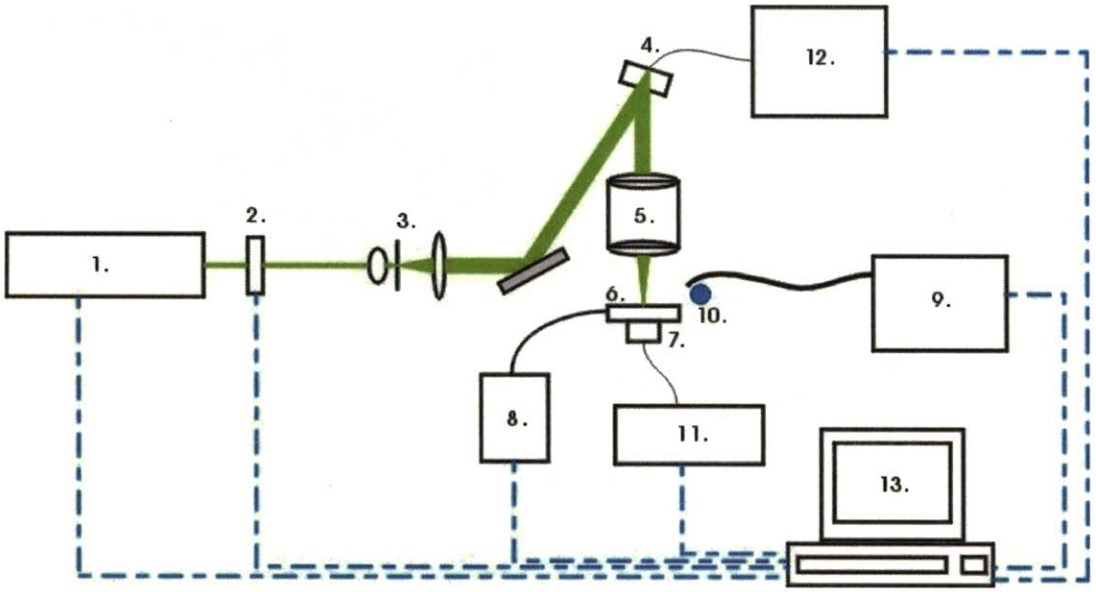

Figure 6.1 Schematic of experimental apparatus

The components that comprise the built system are listed below, corresponding to the labelling of fig.6.1:

1. 15W Argon Ion Laser (Coherent INNOVA 200)
2. Mechanical shutter (Uniblitz)
3. Beam expander / pinhole

4. DMD Micromirror array (Texas Instruments 848 x 600 pixels. 16μm square pixels.)
5. Magnification optics (Melles Griot 3X and 7X lenses)
6. Heated sample stage (Custom)
7. XYZ motorized axis (Newport)
8. PID stage temperature controller (Omega)
9. Syringe pump - material deposition (Braintree Scientific)
10. Draw down bar - material deposition (Custom)
11. XYZ motor controllers (Newport)
12. DMD Micromirror array driver board (Rochester Microsystems)
13. Computer control (Custom scripting software, VB, C++)

The general build scheme being pursued with this apparatus is a micron scale, parallel patterning, variant of stereo-lithography. The route to three dimensional objects is by layering in the mode of figure 6.2. In building many-multi-layered devices fast patterning of each layer is critical in keeping build time realistic - hence the choice of a parallel patterning scheme over a linear scanning method such as those introduced in the previous chapter.

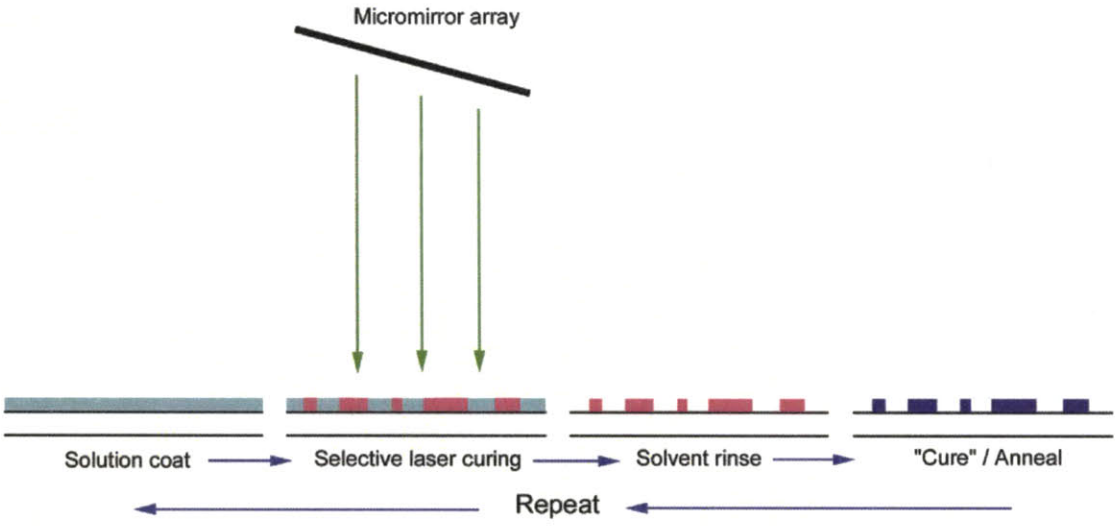

Figure 6.2. Build scheme for patterning via micromirror array.

Optical limitations of apparatus

Micromirror arrays are a silicon MEMS device that suffer the typical MEMS difficulty of stiction due to ambient humidity. For this reason the arrays are sealed behind optical glass. This glass presents a

number of difficulties. Firstly , it absorbs an appreciable amount of incident energy - commercially available arrays absorb highly in the UV - a quartz glass window would alleviate this problem. Secondly, and more importantly, the glass cover contributes to considerable internal reflections at each interface and hence multiple overlapped images are projected from the surface; the primary image, and secondary images at regular intervals in both axes of the horizontal plane. Because the projected images are large in area an aperture is insufficient to eliminate the secondary images unless a very large working distance is used between the mirror array and the magnifying optics. These secondary images are the cause of a significant amount of noise in the projected primary image making high contrast at the interface between on and off pixels difficult. Contrast ratios of 100:1 were typical of this experimental work. This is of more importance when working with the thermally activated nanocrystalline colloids than with photo-chemically sensitized resists as indeed the achieved results indicate. An ideal micromirror array for this type of projected flexible mask work would have no glass coverplate and operate purely as a single reflective surface. Another optical limit in this apparatus is the spatial distribution of light exiting the laser. This is discussed further below.

Digital Apodisation:

The light intensity is spatially varied across the beam exiting the laser, and is further modified by various components in the optical path. This is problematic in the construction method outlined herein because hotspots in the distribution cause localised bleeding of the projected image. Figure 6.3 shows the spatial distribution as written into a silver colloidal film at increasing exposure levels. Figure 6.4 is a measured distribution of this beam as determined by a photo-detector measuring intensity as individual mirrors in the micromirror array are flipped.

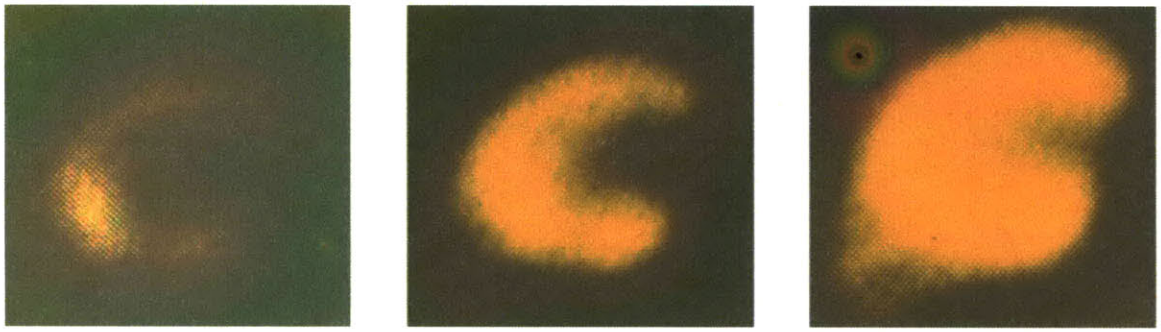

Figure 6.3 Increasing exposure times of raw (unimaged) incident beam on a film of silver nanocrystals demonstrating spatial distribution of energy within the beam.

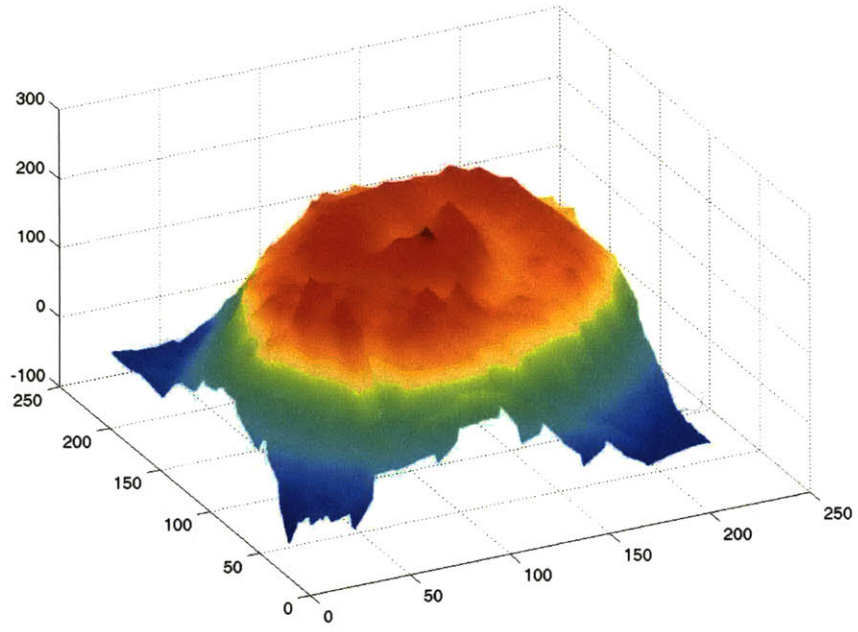

Figure 6.4. Spatial distribution of light intensity as measured with a photocell and selectively displaying individual pixels from the DMD.

It is desirable to remove this light – and hence thermal – distribution from the imaged surface. This was achieved using switching of the micromirror array, or 'digital apodisation'. The residual effects of this distribution can be seen in the test pattern of figure 6.5 a). To achieve curing of a reasonable surface area many areas become over-exposed and thermal bleeding leads to poor image

reproduction in the post-exposure rinsing, and the residual fringes seen in this image.

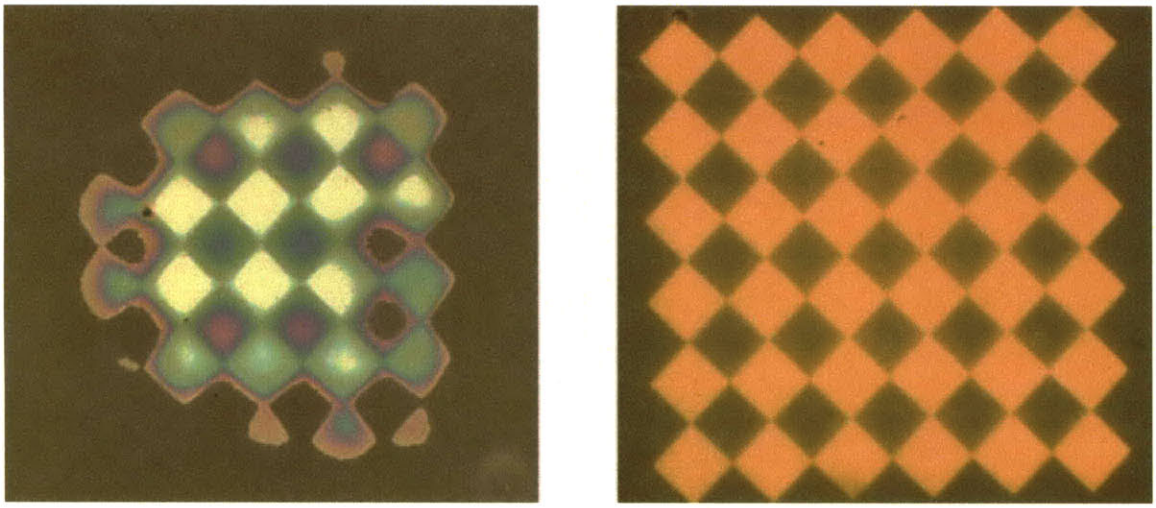

Figure 6.5 Digital apodisation: a) Effect of spatial distribution of light on an exposed and washed pattern. b) Same pattern at same magnification after time modulated apodisation of the image. Note that a larger area can be imaged because overexposure at 'hotspots' is reduced.

Digital apodisation was performed as is demonstrated schematically in figure 6.6. The desired image was broken into multiple images by passing the original image through a filter based on the intensity distribution measured in fig.6.4. The 'hot spot' is iteratively removed from the centre of the image such that the outer extremities of the image will receive the same energy flux as the centre. This process can be performed with 'grey scaling' of the energy flux up to the switching limit of the DMD micromirror array (4kHz). In this work the original image was broken into 16 images, and each image displayed for a time equal to the desired exposure flux at each point.

In further work a more advanced compensation algortihm that also considers thermal transport in the film could be used. As an aside, this technique (which to the author's knowledge has not been published elsewhere) could also be applied to controlled crystal growth or laser recrystallisation, or even studies of thermal transport in

thin films, as the energy input is now temporally and spatially variable.

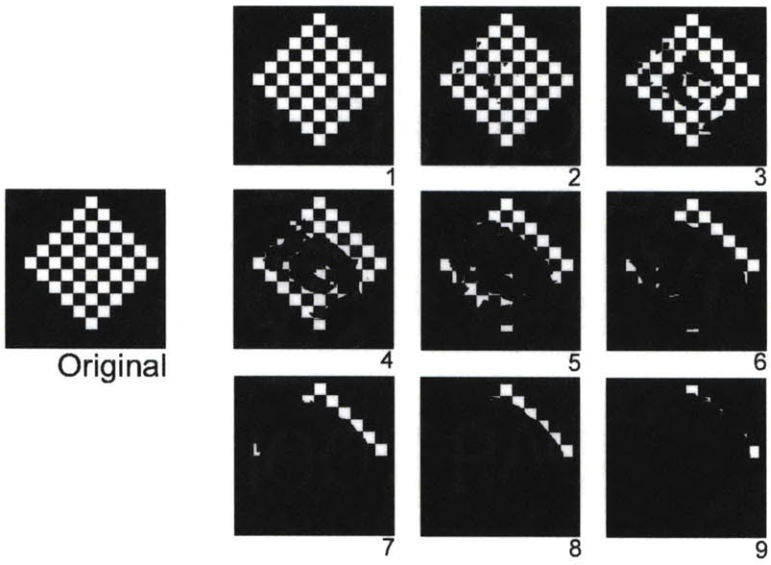

Figure 6.6 Digital apodisation by time varied masking of projected image.

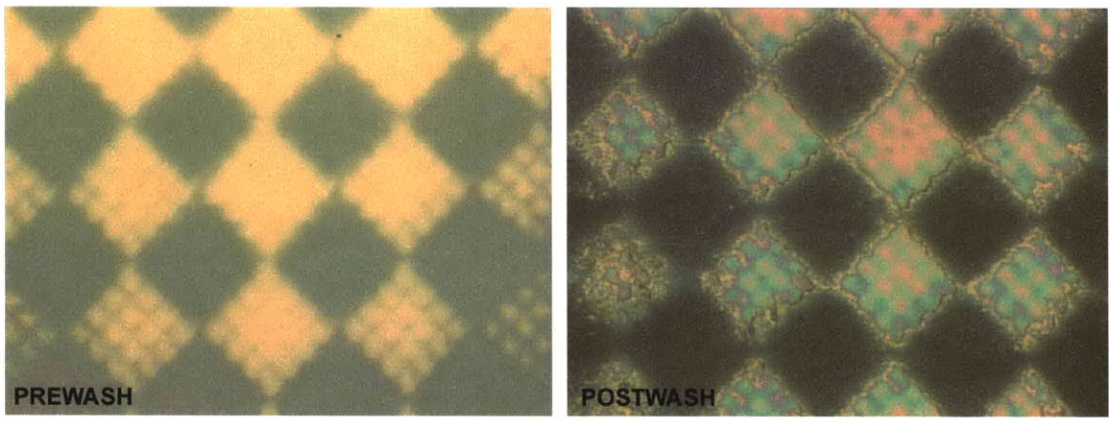

Figure 6.7. Exposed silver before and after a hexane wash.

Patterning of nanocrystalline colloids:

The optical patterning of nanocrystalline materials requires 2 x 10^{-4} $W\mu m^{-2}$ for 10ms exposures 3 x 10^{-5} $W\mu m^{-2}$ for 10s exposures. The much higher total energy flux for the longer exposure is due to thermal dissipation. This indicates that a pulsed excimer laser or other source would be ideal for patterning these materials as low penetration depths and high localised temperatures are possible.

Some of the inherent difficulties with patterning these materials can be seen in figure 6.7. Uneven distribution of incident energy leads to uneven curing. The post-wash image clearly illustrates areas of incomplete curing and incomplete removal of uncured material upon washing with solvent. Further optimisation of both the exposure and rinsing processes is required.

Patterning of photoresists and spin glasses:

Photo resists have a chemically designed non-linearity such that 'waste' light, or optical noise, has a lesser effect than in the exposure of nanocrystals which is thermally determined. The rapid patterning of photo-resists for fast mask production, and the manufacture of polymeric MEMS is a field of growing interest. Particularly in the micro-contact printing effort of my research group, the 1-2 week turn-around time typical for chrome on glass masks is a frustrating limitation in process development. To prove the utility of the apparatus built in this thesis, the patterning of photoresists as a stamp pre-cursor was pursued. Depending on the magnifying optics in the setup, a pixel size (limit of resolution) of 2.2μm or 4.9μm is set. This determines the design rule for MEMS or logic devices fabricated from these masks (and hence stamps).

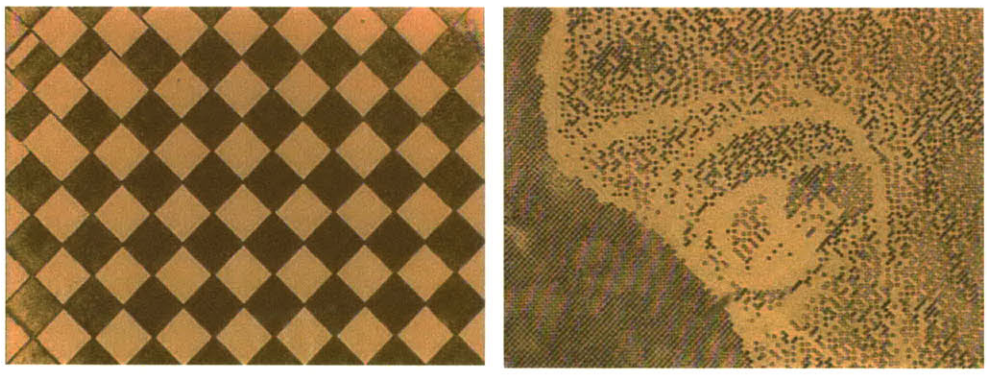

Figure 6.8. Test images in photoresist. a.) 4.9um pixels, 20x20 pixels per square. b.) demonstration of arbitrary design output.

Test images were projected into Shipley negative photoresist (SPR3012) that were spun onto glass slides. Photoresist was

developed in Shipley Microposit developer for 60s. Test images are shown in figure 6.8.

Rapid prototyping of elastomeric stamps for 'nanoembossing'.

A limitation to current work in nanoembossing and other microcontact printing methods is the time required for making the master mold from which stamps are cast. The time limiting steps are the production of photomasks by traditional mask-houses, and the reproduction in photoresist of these masks. This process typically takes between one and two weeks. To this end, the maskless lithography system described above was used in the manufacture of elastomeric stamps.

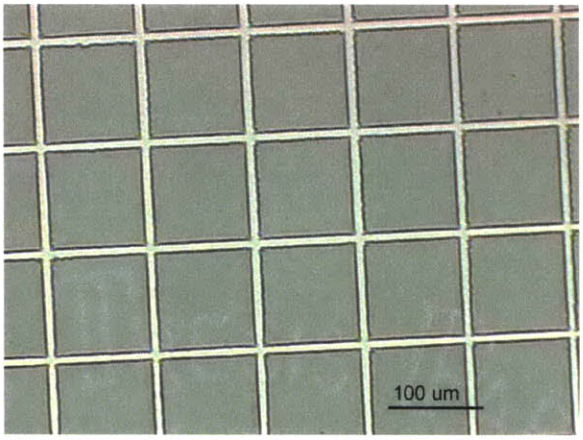

Figure 6.9. A master stamp in photoresist with 10 micron feature sizes. Light areas are clear silicon.

Shipley photoresist (3012) was spun cast on Si wafers and pre-baked at 90°C for 60 seconds. The resist was exposed using collimated light at a wavelength of 532nm (Coherent DPSS 532). CAD designs were projected from the micromirror array utilising the compensating apodisation algorithm described above. Post exposure the resist was developed in Shipley Microposit developer and post-cured at 120°C for 5 minuted. PDMS (Sylgard 182) was poured onto the master and allowed to cure at 70°C for 3 hours before removal as a cured stamp.

Figure 6.9 is a reflected light micrograph of a stamp master. Figures 6.10 & 6.11 a) and b) are transmitted light images of the stamp and printed features respectively.

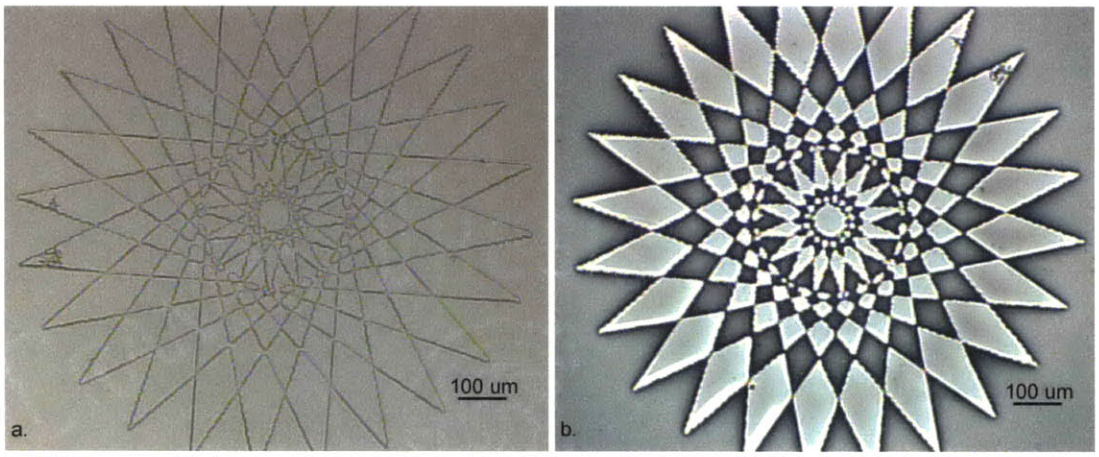

Figure 6.10 a) PDMS stamp cast from micromirror patterned master at a magnification of 2.2X per pixel or 7 micron feature size. c) Corresponding stamped structure in Silver on glass.

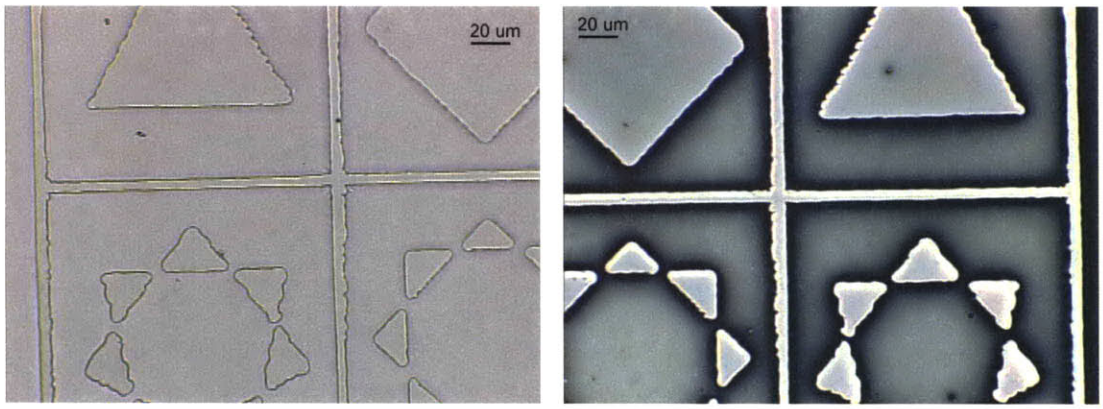

Figure 6.11 a.) PDMS stamp at 5x per pixel or 2.5 micron pixel size. b.) Corresponding stamped structure.

Figure 6.12 is a 50X micrograph of silver printed on glass. Line roughness due to the micromirror array are apparent. One limitation of this patterning technique is the pixelated steps of the bit based micromirror. Linear scanning routes have higher resolution and better line edges at the expense of speed. Conductivity of the patterned silver was demonstrated although not quantified. It is expected to be similar to the results in the previous chapter once the silver has been annealed at 250°C. By this route the fabrication of stamp masters has been reduced from weeks to hours. Large area

stamps can be manufactured by field stitching, and the stamp sizes are no longer limited by wafer and mask size.

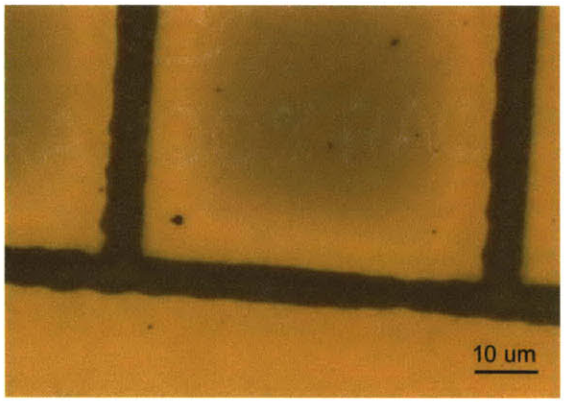

Figure 6.12. 2 pixel wide channels in silver on glass. Reflected light image.

One of the limiting factors in the resolution of this technique was the lack of an adhesion promoter in the application of the photoresist. Whereas in traditional techniques a HMDS pre-bake is employed, no such gas was used in this work. Photoresist could be seen to physically peel from the substrate, particularly around small features.

Summary and further work.

An array of rapid prototyping tools and methodologies have been presented for fabricating printed micro-electromechanical components at the micron scale. In particular, the unique properties of nanocrystalline materials have been exploited in designing faster, and lower cost routes to MEMS. In point form, these novel fabrication techniques and results are:

- Low cost, simple metal film patterning technique using UV patterning, through a chrome on glass mask, of nanoparticles on arbitrary flat surfaces.

- Rudimentary three dimensional nanostructures patterned via electron beam lithography in multiple functional materials.

- The construction of a rapid prototyping platform for the optical patterning of solution based materials to 2.2 micron resolution including a novel method for apodisation of incident coherent light based on switching a micromirror array.

- The first known optical patterning of nanocrystalline colloids and implementation in a rapid prototyping tool.

- Development of a practical mask and stamp writing tool useful in rapid prototyping and development of microcontact printing based technologies and devices.

A flexible experimental apparatus now exists for further exploration of PEMS. Further work in the patterning of multi-layered and multi-material MEMS directly from nanocrystalline precursors remains. The implemented apparatus also allows for further study and utilisation of the nanoembossing technique. Resolution currently stands at 5-6 microns, but is expected to improve with tweaking of the optics and of the photoresist processing including substrate adhesion promoters.

The main gains in this thesis over contemporary rapid prototyping tools was in the exploration of a materials system and processing scheme that conceptually allows for a broad array of materials to be patterned into complex three dimensional parts. Existing rapid prototyping systems are nearly all limited to one or two materials in a single build, and never with a scheme that can incorporate semi-conductors, metals, and dielectric materials, all in the same device. In moving rapid prototyping tools to a truly more flexible material system that can allow logic and other functional devices to be built, an entirely new world of possibilities is apparent. Large area printed electronics, truly 3 dimensional logic and MEMS, and rudimentary printed robots are just some of the new opportunities for development. The move towards the rapid-prototyping of function as opposed to merely structural reproduction is a key shift in this field.

It has been mentioned earlier in this work, but cannot be emphasised enough, that biological systems gain their elegant complexity through layered self-assembly and parallel building processes. The work in this thesis was using a top down approach to building three dimensional structure, specifying each individual voxel and the material therein. This methodology will ultimately hit a limit in the complexity of devices it can manufacture in the same way it is now at the limits of our computational ability to design more complex integrated circuits. Specifying to micron resolution the design file for a 1 cubic centimetre object in 5 materials represents over 1 Terabyte of information - this will quickly becoming an intractable data and material handling problem. The real future of work in this area is in divining the engineering principles behind tiered self assembly and a form of parallel processing that can be applied to designing and building complexity.

Acknowledgements

I would like to thank Brent Ridley, Brian Hubert, Colin Bulthaup, and Eric Wilhelm for helpful discussion during this work. I would also like to sing praise for the ever energetic MIT UROP's, Will DelHagen, Brian Stube, and Denise Cherng for help with hardware and software. I must also thank the many students, academics, staff, and others, of the MIT Media Lab, for creating an undoubtedly stimulating, if somewhat gloriously distracting, environment.

I would also like to thank the readers of this thesis, Professor Hiroshi Ishii, Professor Neil Gershenfeld, and Professor Joseph Jacobson.

Mostly I would like to thank my parents. I thank my father for teaching me that anything can be taken apart, that most things can be fixed, and that some things can be put back together complete. I thank my mother for inspiring, encouraging, and tolerating that process.

I would also like to gratefully acknowledge the fellowship support of LEGO corporation.

References

1. ***BUR93***, Burns, Marshall., Automated Fabrication, PTR Prentice Hall, 1993

2. ***JAC92***, Jacobs, Paul.F., Rapid Prototyping and Manufacturing, SME, 1992

3. ***FEY59***, Feynman, R.P., "There's Plenty of Room at the Bottom", Caltech's "Engineering and Science", February, 1960, www.zyvex.com/nanotech/feynman.html

4. ***EIG90***, Eigler, D.M., Schweizer, E.K., Positioning single atoms with a scanning tunnelling microscope, Nature, 344, 5 April 1990, 524, 1990

5. ***BIN82***, Binnig, G., Rohrer, H., Gerber, Ch. Weibel, E., Applied Physics Letters, 40, 178-180, 1982

6. ***BIN86***, Binnig, G., Quate, C.F., Gerber, Ch., Atomic Force Microscope, Physics Review Letters, 56, No.9, 930, 3-Mar-1996

7. ***DAG90***, Dagata, J.A., Schneir, J., Harrary, H.H., Evans, C.J., Pstek, M.T., Bennet, J., Applied Physics Letters, 56, 2001, 1990

8. ***SUG94***, Sugimura, H., Uchida, T., Kitamura, N., Mashuhara, H., J.Phys.Chem., 98, 4352, , 1994

9. ***COO99***, Cooper, E.B., Manalis, S.R., Fang, H., Dai, H., Matsumoto, K., Minne, S.C., Hunt, T., Quate, C.F., Terabit-per-square-inch data storage with the atomic force microscope, Applied Physics Letters, 75(22), 3566, Nov-99

10. ***WIL97***, Wilder, K., Soh, H.T., Atalar, A., Quate, C.F., Hybrid atomic force / scanning tunneling lithography, J.Vac.Sci.Technol.B, 15(5), 1811, Sep/Oct 1997

11. ***WIL98***, Wilder, K., Quate, C.F., Singh, B., Kyser, D.F., Electron beam and scanning probe lithography: A comparison, J.Vac.Sci.Technol.B, 16(6), 3864, Nov/Dec 1998

12. ***HUB00***, Hubert, Brian. N., Private communications, 2000

13. ***PIN99***, Piner, R.D., Zhu, J., Xu, F., Hong, S., Mirkin, C.A., "Dip Pen" Nanolithography, Science, 283, 661, 1999

14. ***XIA98***, Xia, Y., Whitesides, G.M., Soft Lithography, Angew. Chem. Int Ed., 1998 (37) 550.

15. ***NON98***, Nonogaki, S., Takumi, U., Toshio, I., Microlithography fundamentals in semiconductor devices and fabrication technology, Marcel Dekker, 1998

16. ***FUL00***, Fuller, Sawyer Buckminster., Ink Jet Deposition of Inorganic Nanoparticle Materials as a Route to Desktop Fabrication of Integrated Logic and Micromachinery, Thesis., Bachelor of Science in Mechanical Engineering., Massachusetts Institute of Technology, Jun-00

17. ***WIL90***, Williams, Paul A., Three Dimensional Printing: A new process to fabricate prototypes directly from cad models., Master's thesis., Massachusetts Institute of Technology, 1990

18. ***PAP84***, Papanek, Victor, "Design for the real world: Human Ecology and Social Change", 2nd Ed. New York, Van Nostrand Reinhold, 1984

19. ***PAP92,*** Papanek, Victor, "The green imperative: Ecology and Ethics in Design and Architecture", New York, Thames and Hudson, 1995.

20. ***TAK00***, Takeuchi, Shoji., A three-dimensional shape memory alloy microelectrode with clipping structure for insect neural recording., Journal of Microelectromechanical Systems, 9.No.1., 24, IEEE, 2000

21. ***LEV93***, Levy, Steven., Artificial Life: A report from the frontier where computers meet biology, Vintage Books , 1993

22. ***TSA99***, Tsao, Che-Chih, Sachs, Emanuel., Photo-Electroforming: 3-D Geometry and Materials Flexibility in a MEMS fabrication process., , , IEEE Journal of Microelectromechanical Systems, 8.No.2, 161, IEEE, 1999

23. ***MAK98***, Makino, Eiji., Shibata, Takayuki., Micromachining compatible metal patterning technique using localized decomposition of an organometallic compound by laser irradiation., J.Micromech.Microeng., 8, 177-181, 1998

24. ***MUL97***, Mullenborn, M., Grey, F., Bouwstra, S., Laser direct writing on structured substrates, J.Micromech.Microeng., 7, 125-127, 1997

25. ***MAR98***, Maruo, Shoji., Kawata, Satoshi., Two Photon Absorbed Near Infrared Photopolymerization for three dimensional microfabrication, Journal of Microelectromechanical Systems, 7.No.4., 411, IEEE, 1998

26. ***FOL99***, Folch, Albert., Schmidt, Martin.A., Wafer-Level In-Registry Microstamping, IEEE Journal of Microelectromechanical Systems, 8.No.1., 85, IEEE, 1999

27. ***COH99***, Cohen et al, EFAB: Low-Cost, Automated Electrochemical Batch Fabrication of Arbitrary 3-D Microstructures, Micromachining and Microfabrication Process Technology, SPIE 1999 Symposium on Micromachining and Microfabrication, Santa Clara, CA, September 22, 1999.,

28. ***BUF76***, P Buffat, JP Borel, Physical Review A, 1976 (13) 6, 2287

29. ***GOL91***, AN Goldstein, VL Colvin, AP Alivisatos, Mat Res Soc Symp Proc, 1991 (206), pp271

30. ***GOL96***, AN Goldstein, Applied Physics A, 1996 (62) 1, pp33

31. ***GOL92***, AN Goldstein, CM Echer, AP Alivisatos, Science, 1992 (256), pp1425

32. ***ZEN98***, Zeng, P., Zajac, S., Clapp, P.C., Rifkin, J.A., Nanoparticle sintering simulations, Materials Science and Engineering , A252, 301-306, 1998

33. ***ERC91***, F Ercolessi, W Andreoni, E Tosatti, Physical Review Letters, 1991 (66) 7, 911

34. ***RID99***, Ridley, Brent, Inorganic Semiconductors for Printed Transistors, Thesis, Masters thesis, Massachusetts Institute of Technology, 1999

35. ***LAN96***, Lange, F.F., Chemical Solution Routes to Single-Crystal Thin Films, Science, 273, 16 August, 903, 1996

36. ***SCH97***, DL Schultz, CJ Curtis, RA Flitton, H Wiesner, J Keane, RJ Matson, PA Parilla, R Noufi, DS Ginley., NREL/SNL Photovoltaics Review, 1997 683.

37. ***CLA97***, Clarke, L., Wybourne, M.N., Yan, M., Cai, S.X., Keana, J.F.W., Transport in gold cluster structures defined by electron-beam lithography, Applied Physics Letters, 71(5), 617, Aug-97

38. ***HOF93***, Hoffman, P., Assayag, G.Ben, Gierak, J., Flicstein, J., Maar-Stumm, M., Van Den Bergh, H., Direct writing of gold nanostructures using a gold-cluster compound and a focused ion beam., J. Appl. Phys., 74(12), 7588, , 15-Dec-93

39. ***BER95***, Berry, G.J., Cairns, J.A., Thomson, J., New material for the production of fine line interconnects in integrated circuit technology, Journal of Materials Science letters, 14, 844-846, 1995

40. ***BED99***, Bedson, T.R., Nellist, P.D., Palmer, R.E., Wolcoxon, J.P., Direct electron beam writing of nanostructures using passivated gold clusters, in review 1999.

41. ***REE97***, Reetz, M.T., Winter, M., Dumpich, G., Lohau, J., Friedrichowski, S., Fabrication of Metallic and Bimetallic Nanostructures by Electron Beam Induced metallization of surfactant Stabilized Pd and Pd/Pt Clusters, J.Am.Chem.Soc., 119, 4539-4540, 1997

42. **SHV00**, Shvartsburg, A.A., Jarrold, M.F., Solid Clusters above the Bulk Melting Point. Physical Review Letters, Vol.85, Issue 12, pp.2530-2532, 2000.